Introduction to Calorimeters

David Cockerill Southampton Lecture 4 May 2016

Overview

- Introduction
- Electromagnetic Calorimetry
- Hadron Calorimetry
- Jets and Particle Flow
- Future directions in Calorimetry
- Summary

Calorimetry

One of the most important and powerful detector techniques in experimental particle physics

Two main categories of Calorimeter:

Electromagnetic calorimeters for the detection of

$e^{\pm}$ and neutral particles γ

Hadron calorimeters for the detection of

$\pi^{\pm}$, $p^{\pm}$, $K^{\pm}$ and neutral particles n, K^0_L

$\mu^{\pm}$ usually traverse the calorimeters losing small amounts of energy by ionisation

The 13 particle types above completely dominate the particles from high energy collisions reaching and interacting with the calorimeters

All other particles decay ~instantly, or in flight, usually within a few hundred microns from the collision, into one or more of the particles above

Neutrinos, and neutralinos, χ^o, undetected but with hermetic calorimetry can be inferred from measurements of missing transverse energy in collider experiments

Calorimeters

Calorimeters designed to stop and fully contain their respective particles
'End of the road' for the incoming particle

Measure - **energy** of incoming particle(s) by total absorption in the calorimeter
- **spatial location** of the energy deposit
- (sometimes) **direction** of the incoming particle

Convert energy E of the incident particle into a detector response S

Detector response S $\propto$ E

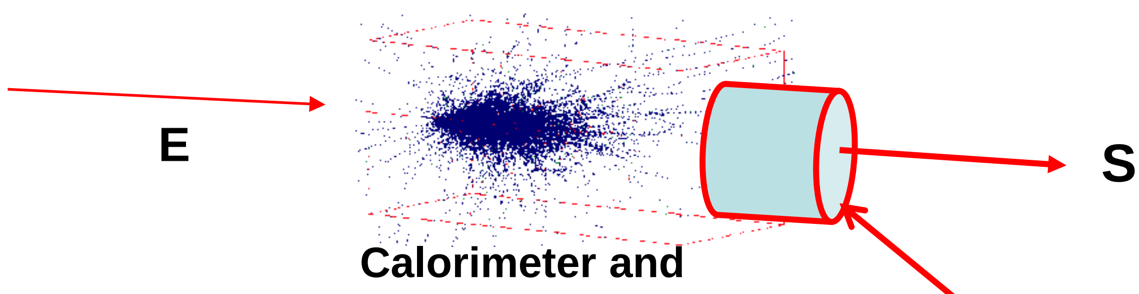

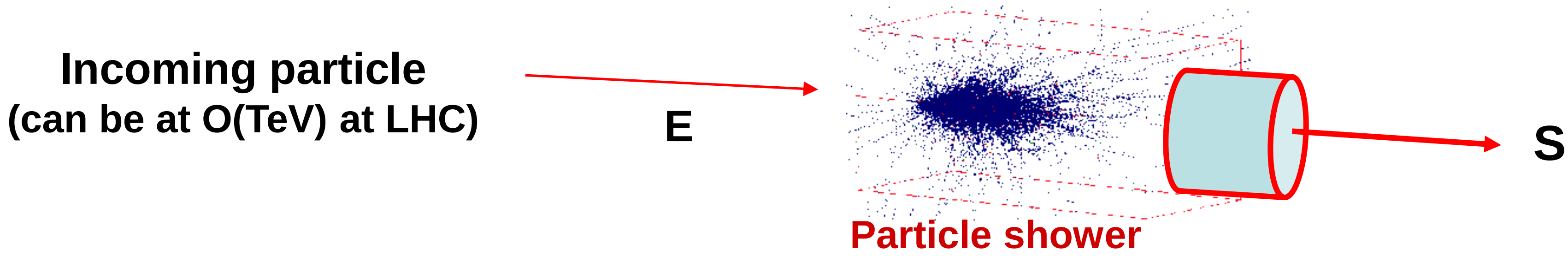

Calorimetry: basic mechanism

Energy lost by the formation of electromagnetic or hadronic cascades /showers in the material of the calorimeter

Many charged particles in the shower

The charged particles ionize or excite the calorimeter medium

The ionisation or excitation can give rise to:

- **The emission of visible photons, O(eV), via scintillation**
- **The release of ionisation electrons, O(eV)**

Photo-detectors or anodes/dynodes then detect these "quanta"

Where you STOP is what you ARE !!!

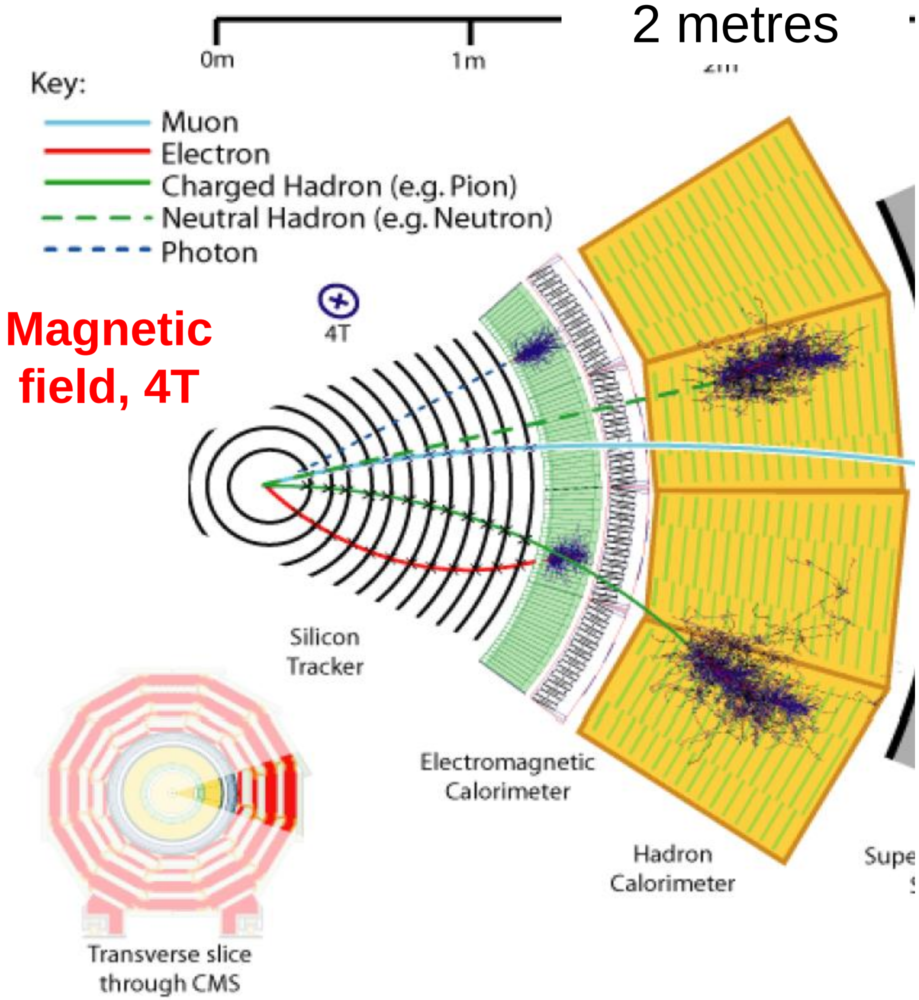

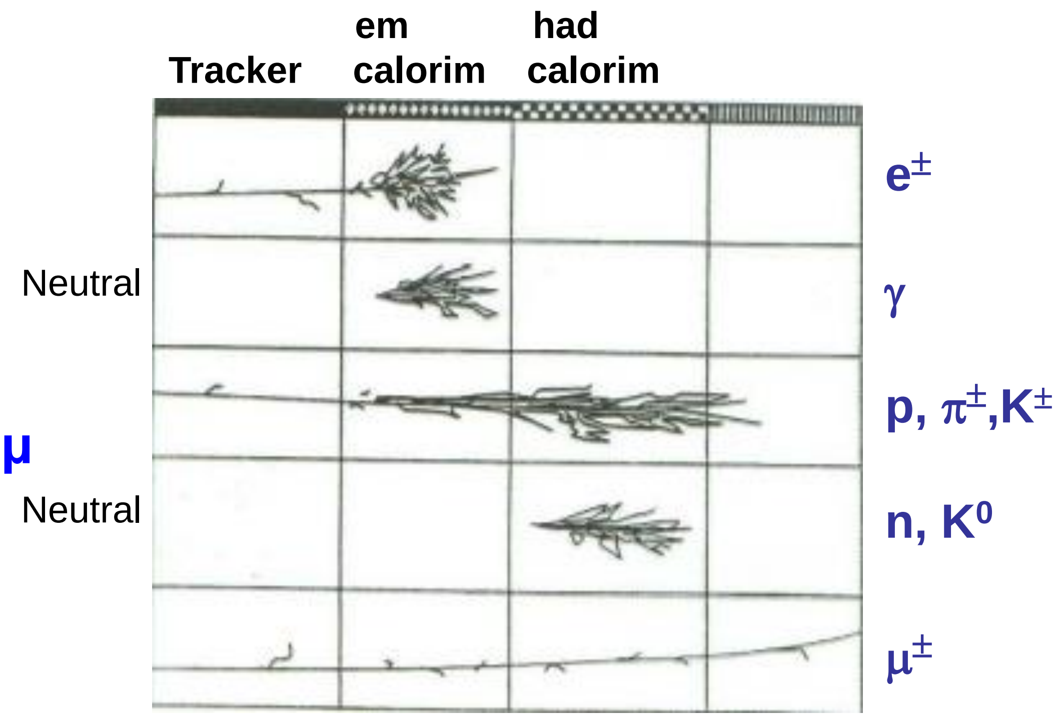

Get sign of charged particles from the Tracker

A 'wedge' end on view of the CMS experiment at the LHC

Tracker to be of minimum material to avoid losing particle energy before the calorimeters.

There are two general types of calorimeter design:

1) Sampling calorimeters

Layers of passive absorber (ie Pb or Cu) alternating with active detector layers such as plastic scintillator, liquid argon or silicon

→ Only part of the energy is sampled
→ Used for both electromagnetic and hadron calorimetry
→ Cost effective

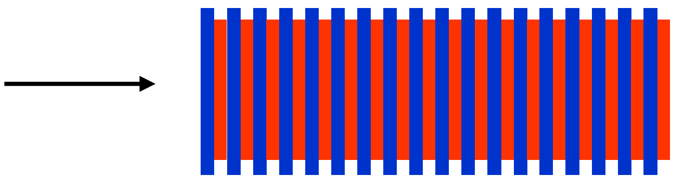

ATLAS	ECAL & HCAL
ALICE	EMCAL
CMS	HCAL
LHCb	ECAL

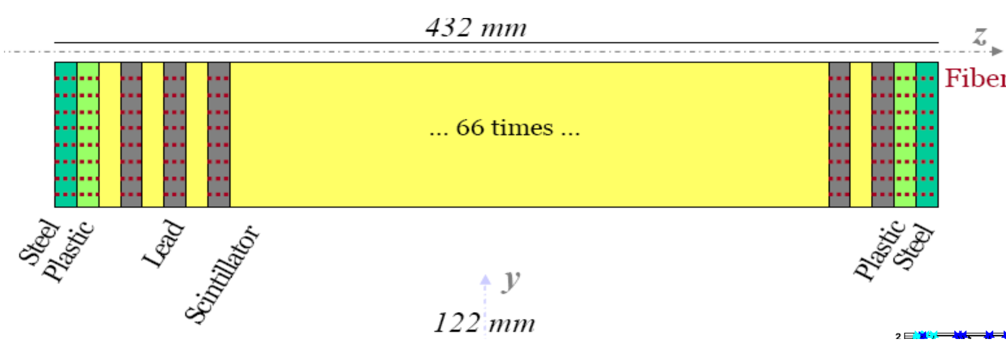

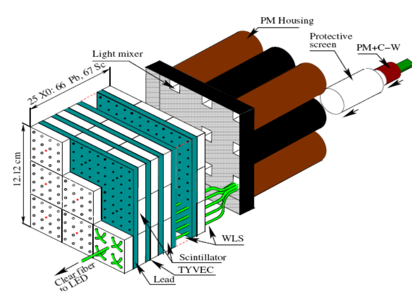

2) Homogeneous calorimeters

Single medium, both absorber and detector

- Liquified Ar/Xe/Kr
- Organic liquid scintillators, large volumes, Kamland, Borexino, Daya Bay
- Dense crystal scintillators: **$PbWO_4$,** CsI(Tl), BGO and many others
- Lead loaded glass

Almost entirely for electromagnetic calorimetry

Babar ECAL CsI(Tl)
ALICE ECAL ($PbWO_4$)

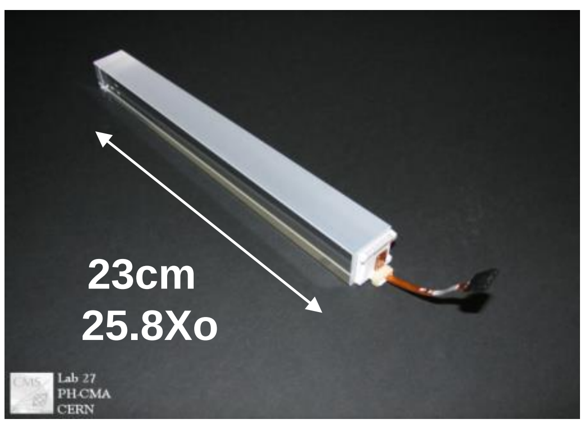

CMS ECAL ($PbWO_4$)

Electromagnetic Calorimetry

Electromagnetic Cascades

Electromagnetic cascades

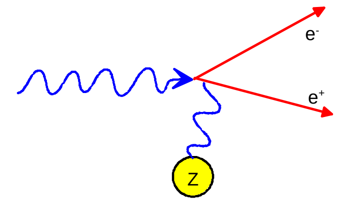

- e± bremsstrahlung and photon pair production

  By far the most important processes for energy loss
  by electrons/positrons/photons with energies above 1 GeV
  Leads to an e.m. cascade or shower of particles

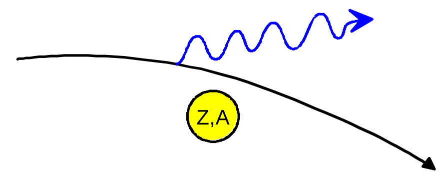

- Bremsstrahlung

  Characterised by a 'radiation length', X_o, in the absorbing medium over which an electron loses, on average, 63.2% of its energy by bremsstrahlung.

$1/m_e^2$ dependence

$$E = E_0 \, e^{-x/X_0}$$

where

$$-\frac{dE}{dx} = 4\alpha N_A \frac{Z^2}{A} r_e^2 E \ln \frac{183}{Z^{1/3}} \quad \Rightarrow \quad -\frac{dE}{dx} \propto \frac{Z^2 E}{m_e^2}$$

$$-\frac{dE}{dx} = \frac{E}{X_0}$$

$$X_0 = \frac{A}{4\alpha N_A Z^2 r_e^2 \ln \frac{183}{Z^{1/3}}}$$

Use high Z materials for compact e.m. calorimetry

$X_0 \sim 180\, A/Z^2$ [g cm^{-2}]

In Pb (Z=82) $X_0 \sim 5.6$ mm

Due to the $1/m^2$ dependence for bremsstrahlung, muons only emit significant bremsstrahlung above ~1 TeV ($m_\mu \sim 210\, m_e$)

Pair production

Characteristic mean free path before pair production, $\lambda_{pair} = 9/7\ X_o$

$$E_\gamma \geq 2m_e c^2$$

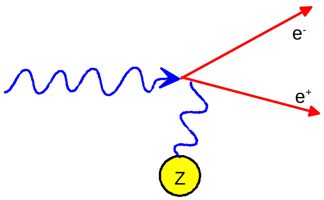

Intensity of a photon beam entering calorimeter reduced to 1/e of the original intensity, $I = I_o \exp(-7/9\ x/X_o)$. $\lambda_{pair} = 7.2$ mm in Pb

Brem and pair production dominate the processes that degrade the incoming particle energy

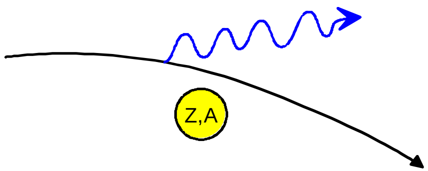

50 GeV electron

Loses 32 GeV over 1 X_0 by bremsstrahlung

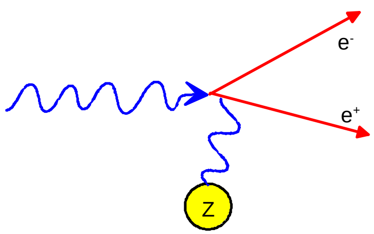

50 GeV photon

Pair production to e+ e- , 25 GeV to each particle

Energy regime degraded by 25 GeV

Minimum ionising particle (m.i.p)

In Pb, over 1 X_0, ionization loss ~O(10s) of MeV

Factor of ~1000 less than the above

Below a certain critical energy, E_c :

e± energy losses are greater through ionisation than bremsstrahlung

The multiplication process runs out

- **Slow decrease in number of particles in the shower**
- **Electrons/positrons are stopped**

Photons progressivley lose energy by compton scattering, converting to electrons via the photo-electric effect, and absorption

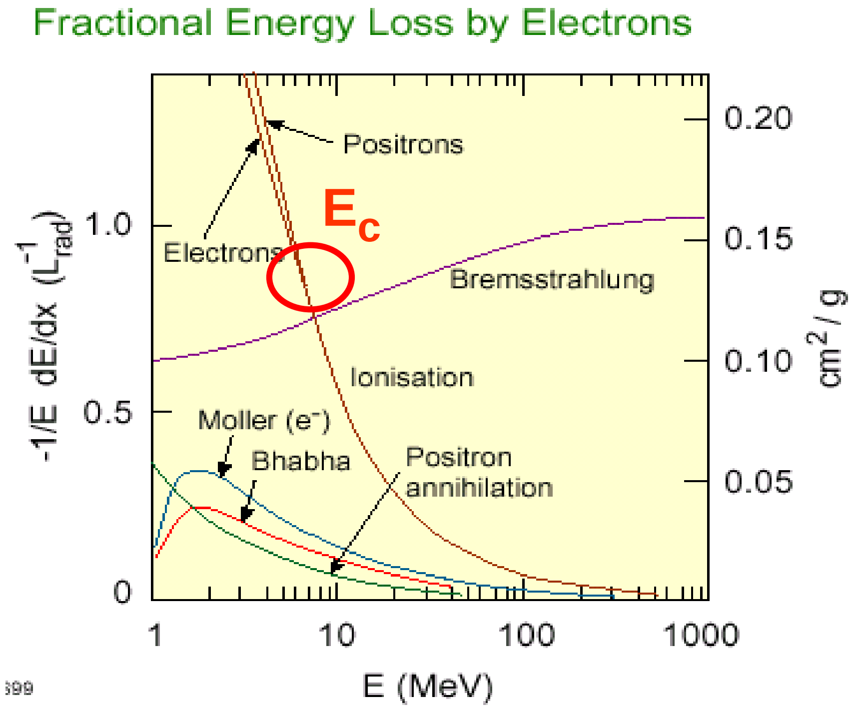

$$E_c \approx \frac{610 MeV}{Z + 1.24}$$

Liquids and solids

Pb (Z=82), **E_c = 7.3 MeV**

EM Cascades: a simple model

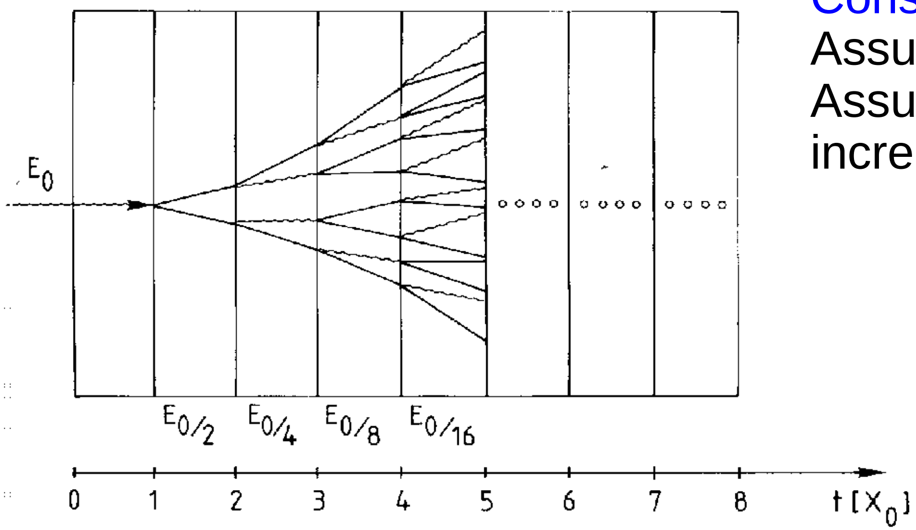

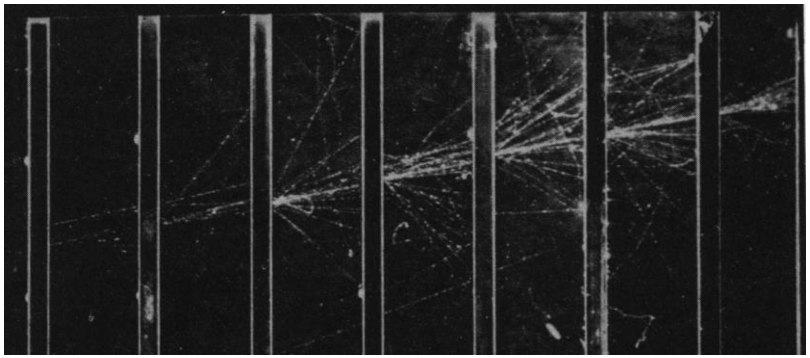

Electron shower in a cloud chamber with lead absorbers

Consider only Bremstrahlung and pair production

Assume: Incident energy = E_0, λ_{pair} and X_0 are equal

Assume: after each X_0, the number of particles increases by factor 2

After 't' layers, each of thickness X_0:

Number of particles = $N(t) = 2^t$

Average energy per particle = $E(t) = E_0 / 2^t$

Process continues until $E(t) < E_c$

This layer contains the maximum number of particles:

$$t_{\max} = \frac{\ln E_0 / E_c}{\ln 2}$$

$$N^{total} = \sum_{t=0}^{t_{\max}} 2^t = 2^{(t_{\max}+1)} - 1 \approx 2 \cdot 2^{t_{\max}} = 2\frac{E_0}{E_c}$$

For a 50 GeV electron on Pb

***N^{total}* ~ 14000 particles**

***t_{max}* at ~13 X_o (an overestimate)**

EM shower development in Krypton (Z=36, A=84)

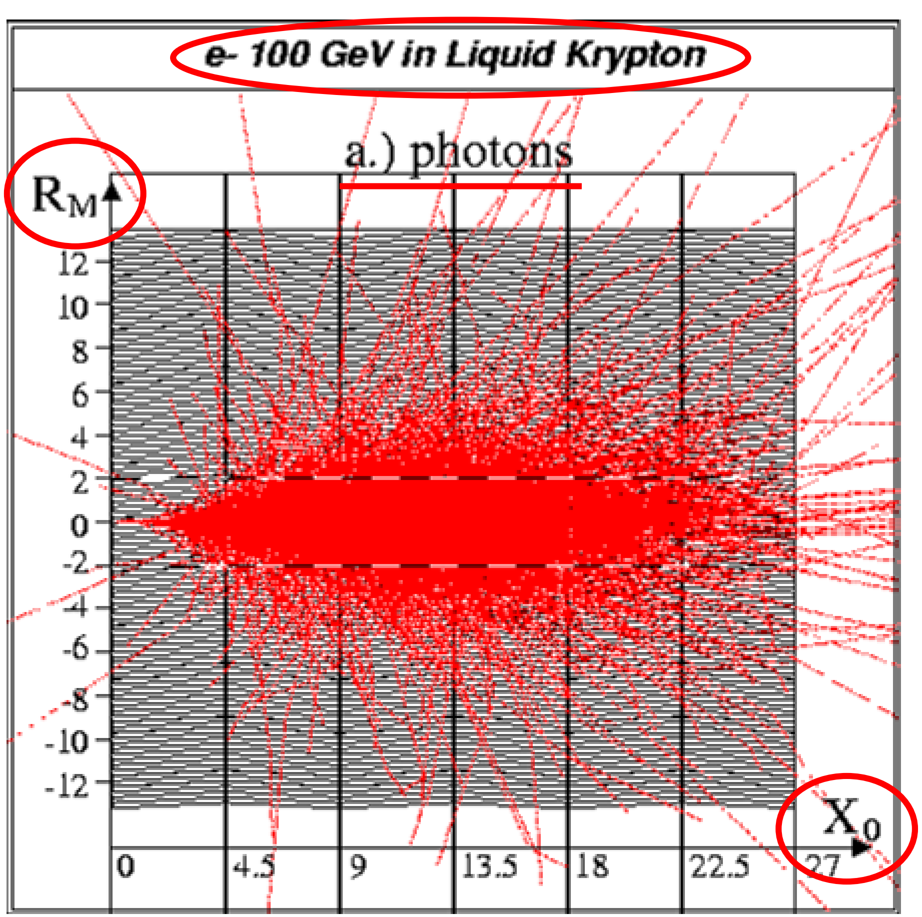

Photons created

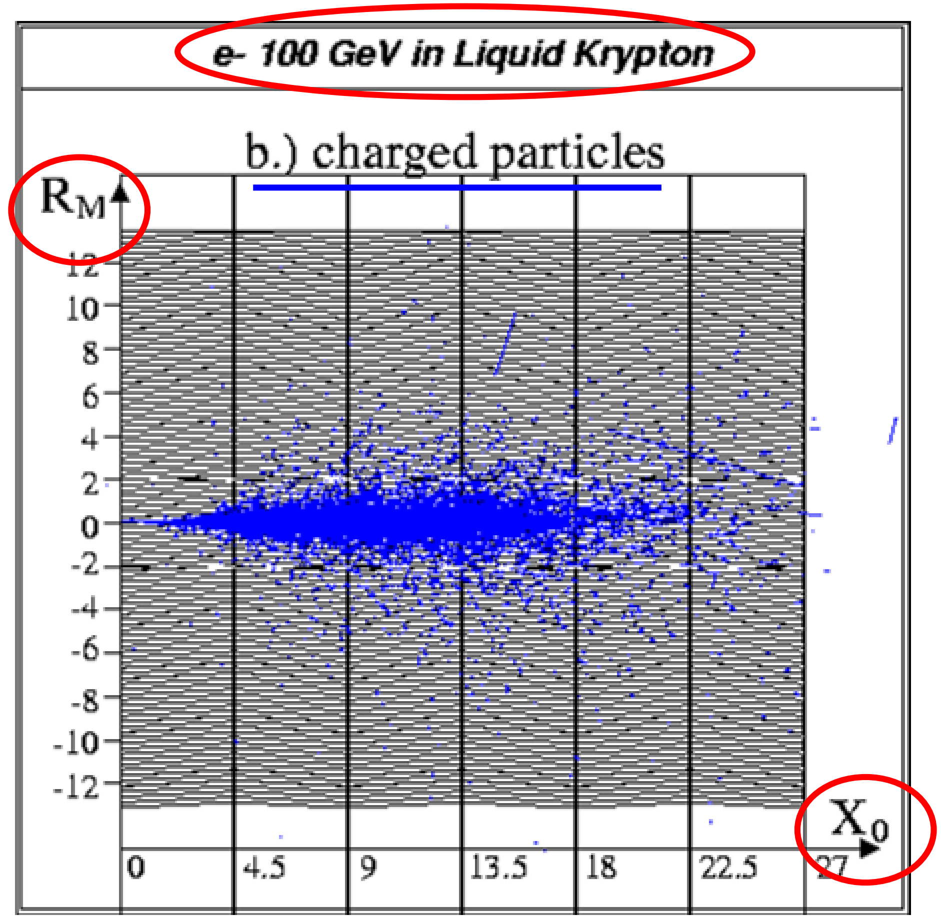

Charged particles created

GEANT simulation: 100 GeV electron shower in the NA48 liquid Krypton calorimeter

EM Cascade Profiles

Longitudinal Shower Development

Shower only grows logarithmically with E_o

Shower maximum, where most energy deposited,

$t_{max} \sim \ln(E_o/E_c) - 0.5$ for $e^{\pm}$

$t_{max} \sim \ln(E_o/E_c) + 0.5$ for γ

$t_{max} \sim 5\ X_o = 4.6$ cm for 10 GeV electrons in $PbWO_4$

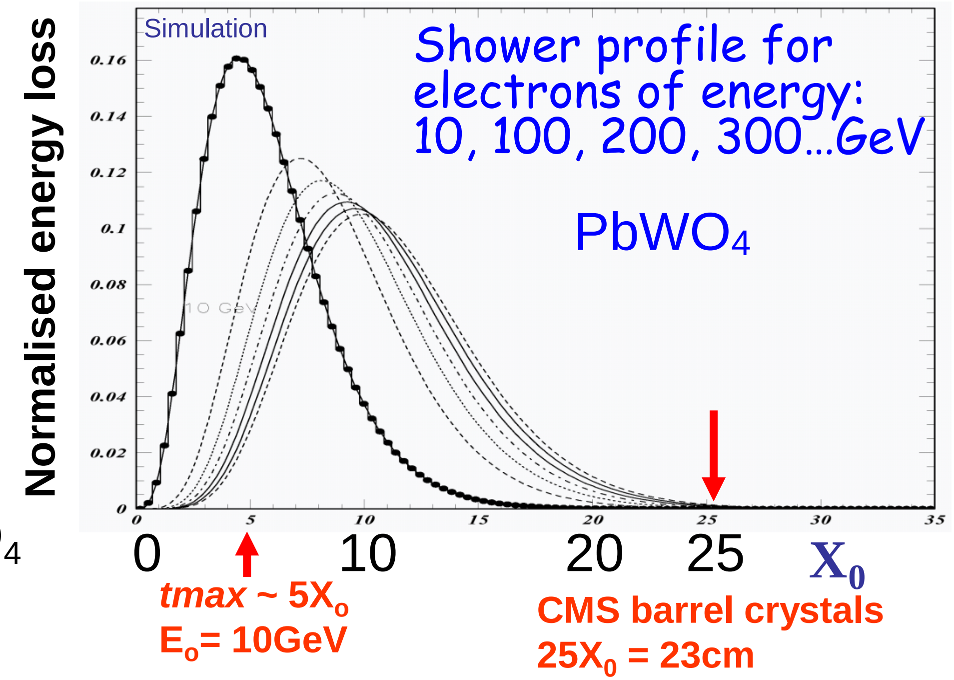

How many X_0 to adequately contain an em shower within a crystal?

Rule of thumb: RMS spread in shower leakage at the back

~ 0.5 * average leakage at the back

CMS requires the rms spread on energy measurement to be < 0.3%

Therefore require leakage < 0.65%

Therefore crystals must be 25 X_0 = 23 cm long

EM Cascade Profiles

Transverse Shower Development

Mainly multiple Coulomb scattering by $e^{\pm}$ in shower

- 95% of shower cone located in cylinder of radius 2 R_M where R_M = Moliere Radius

$$R_M = \frac{21\,\text{MeV}}{E_c} X_0 \quad [g/cm^2]$$

R_M = 2.19 cm in $PbWO_4$
using X_o = 0.89 cm and E_c ~ 8.5 MeV

50 GeV e- in $PbWO_4$

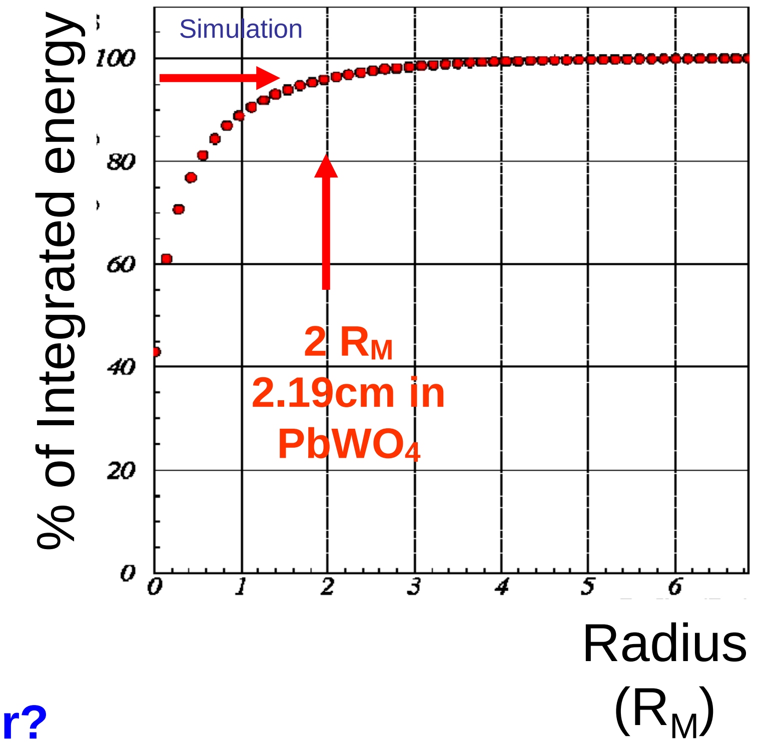

How many R_M to adequately measure an em shower?

Lateral leakage degrades the energy resolution

In CMS, keep contribution to < 2%/sqrt(E)
Achieved by summing energy over 3x3 (or 5x5) arrays of $PbWO_4$ crystals

Detectors for Electromagnetic Calorimetry

$PbWO_4$ crystals: CMS and ALICE

Vital properties for use at LHC:

Compact and radiation tolerant

Density	8 g/cc
X_0	0.89 cm
R_M	2.2 cm

Sum over 3x3 or 5x5 crystals

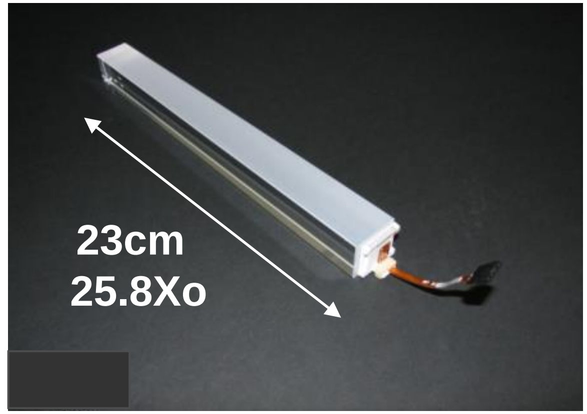

CMS Barrel crystal, tapered ~2.6x2.6 cm² at rear
Avalanche Photo Diode readout, gain = 50

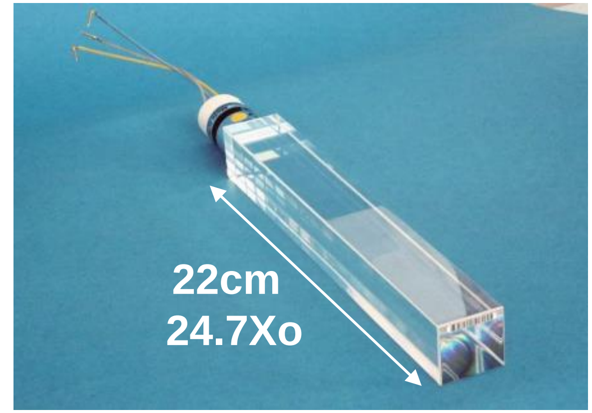

CMS Endcap crystal, tapered, 3x3 cm² at rear
Vacuum Photo Triode readout, gain ~ 8

Fast scintillation

Emission	~80% in 25 ns
Wavelength	425 nm
Output	150 photons / MeV (low, only 1% wrt NaI)

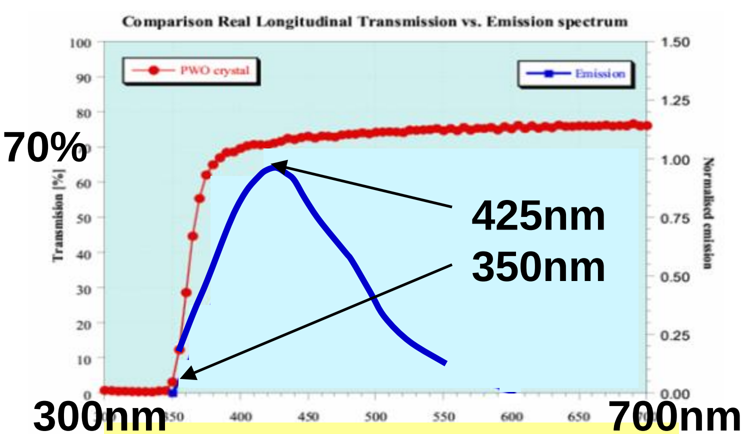

Emission spectrum (blue) and transmission curve

A CMS $PbWO_4$ crystal 'boule' emerging from its 1123°C melt

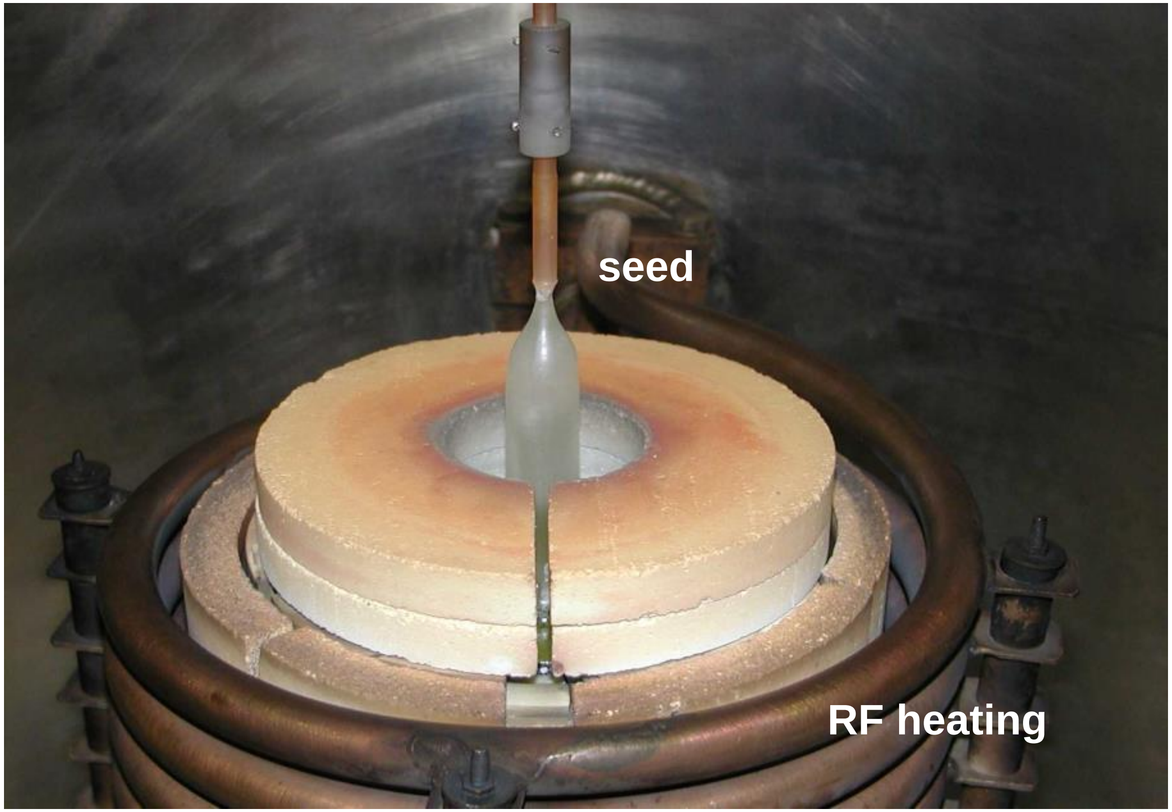

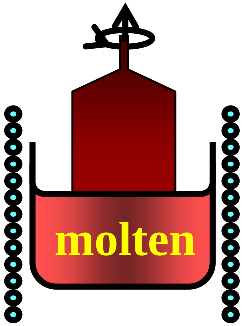

Czochralski method

CMS at the LHC – scintillating $PbWO_4$ crystals

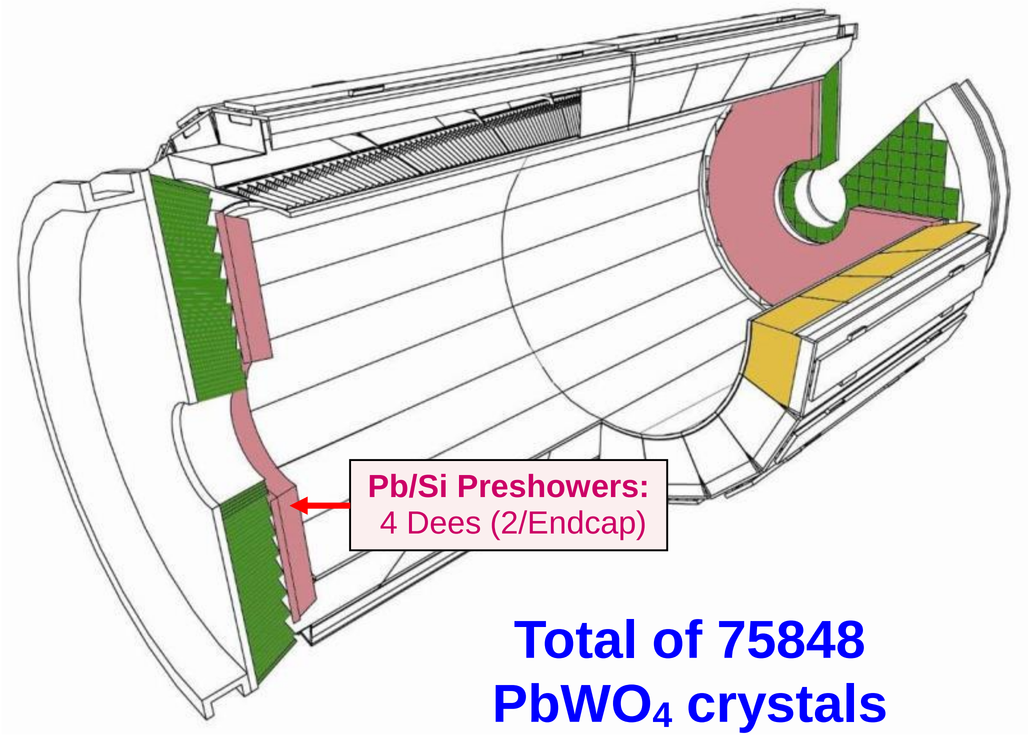

Total of 75848 $PbWO_4$ crystals

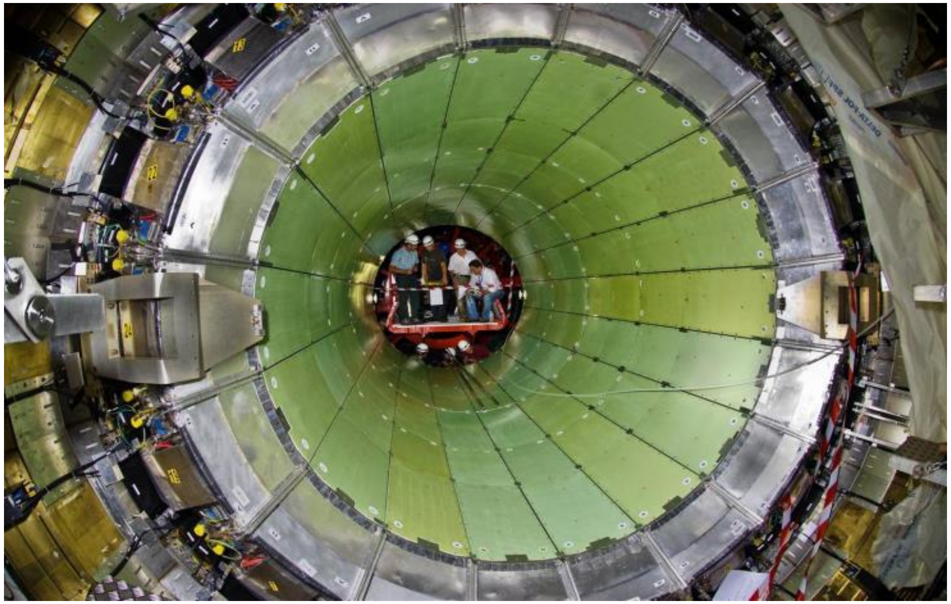

CMS Barrel

Barrel: 36 Supermodules (18 per half-barrel)
61200 Crystals (34 types) – total mass 67.4 t

Endcaps: 4 Dees (2 per Endcap)
14648 Crystals (1 type) – total mass 22.9 t

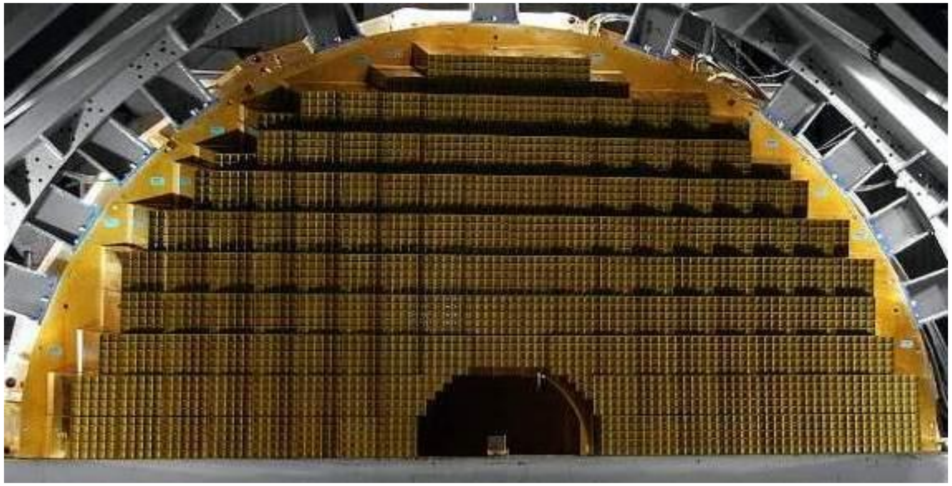

An endcap Dee, 3662 crystals awaiting transport

ATLAS ‘Accordion’ sampling liquid argon calorimeter at the LHC

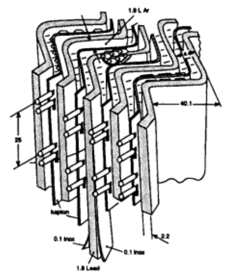

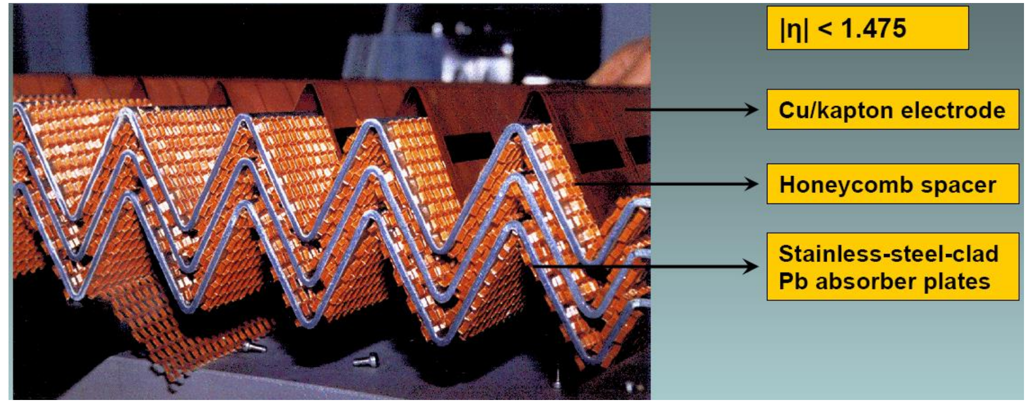

Corrugated stainless steel clad Pb absorber sheets,1-2 mm thick

Immersed in liquid argon (90K)

Accordion geometry minimises dead zones

Liquid argon intrinsically radiation hard

Readout board allows fine segmentation (azimuth, rapidity, longitudinal)

Multilayer Cu-polyimide readout boards

Collect ionisation electrons with an electric field across 2.1 mm liquid Argon drift gap

1 GeV energy deposit → collect 5.10^6 e$^-$

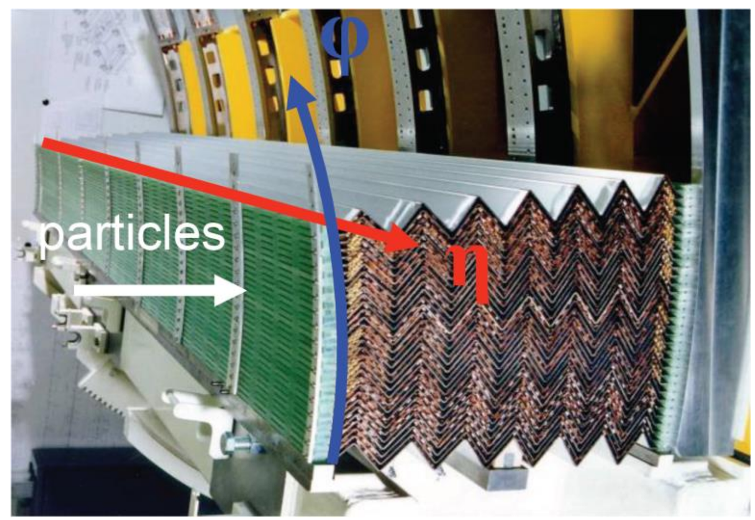

The LHCb sampling electromagnetic calorimeter at the LHC

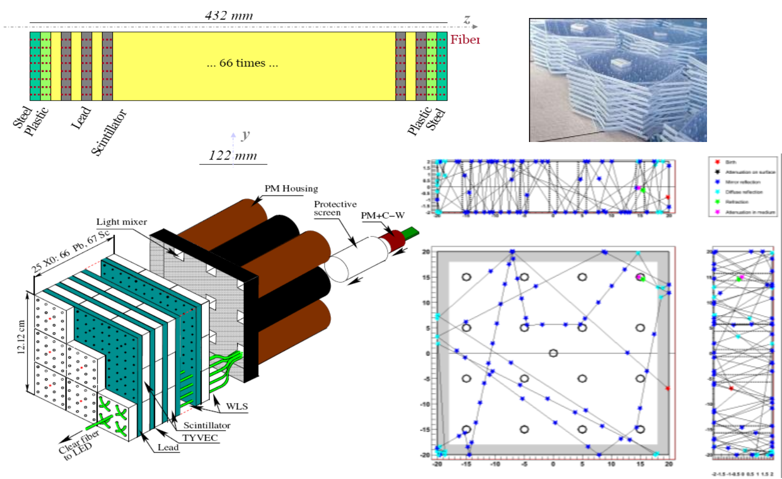

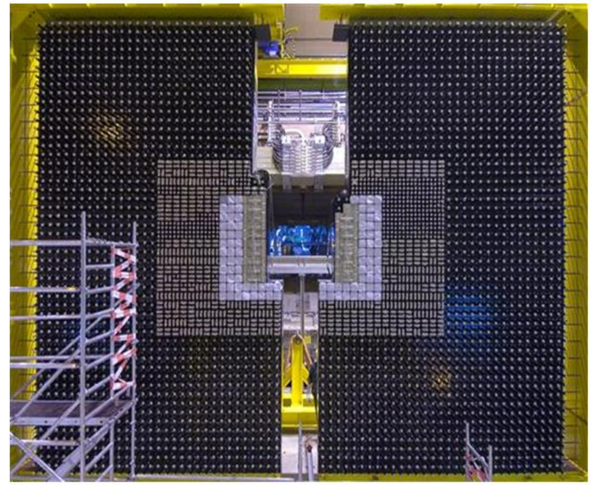

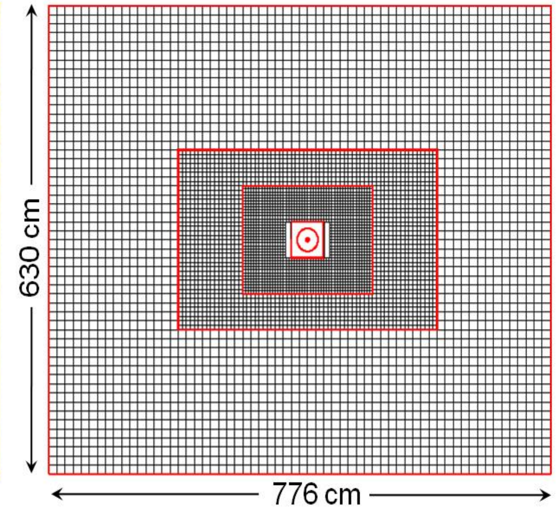

Wall of 3312 modules

LHCb module

67 scintillator tiles, each 4 mm thick
 Interleaved with 66 lead plates, each 2 mm thick

Readout through wavelength shifting fibres
running through plates to Avalanche Photodiodes

3 types of modules

Borexino

Detect 0.862 MeV neutrinos from ^{7}Be decays in the sun

300 t ultra pure organic liquid scintillator. Less than 10^{-16} g/g of ^{238}U and ^{232}Th

10^{4} photons / MeV at 360 nm

3 ns decay time

Photon mean free path 8 m

Readout

2,212 photo-multiplier 8 inch tubes

Timing 1 ns

Cluster position resolution 16 cm

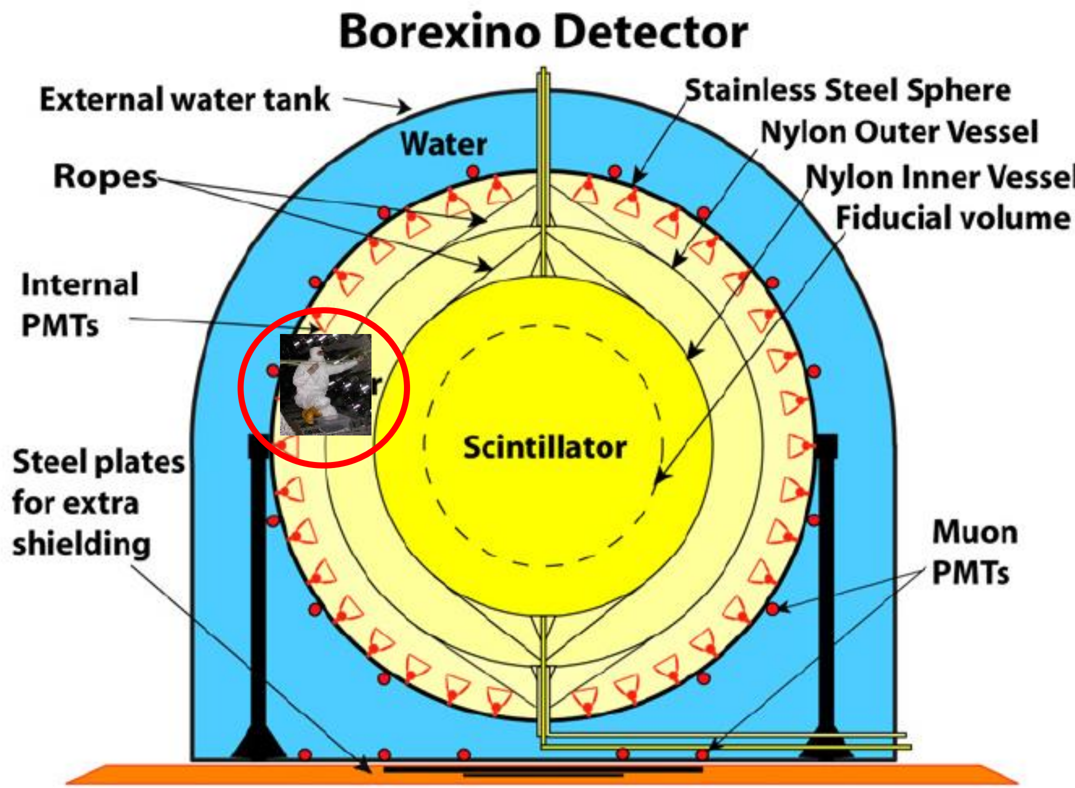

Inner sphere, 4.25 m radius

Outer vessel 5.5 m radius

Steel holding vessel 6.85 m radius

Liquid Scintillator Calorimeters

Borexino

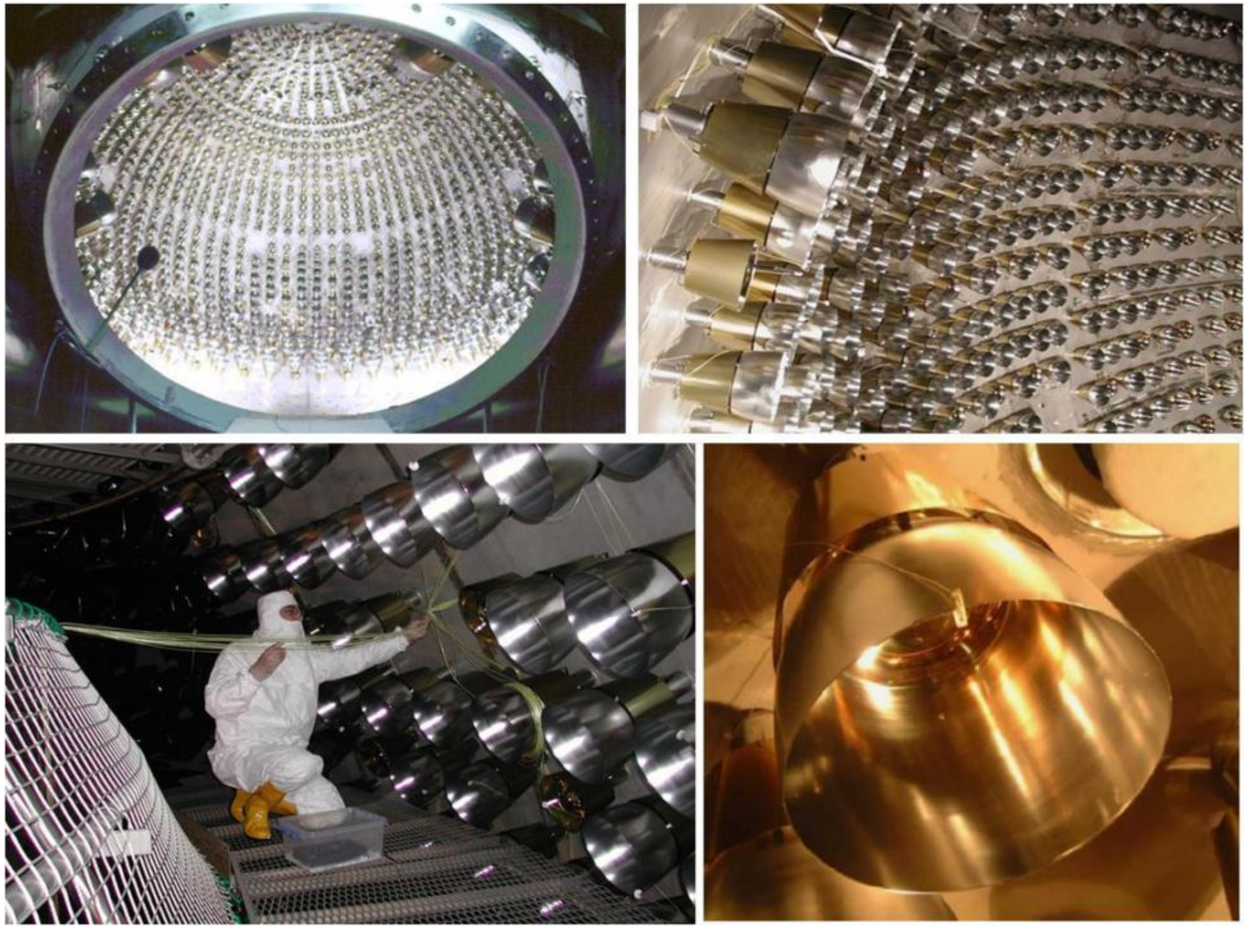

Top: Internal surface of stainless steel support sphere + PMTs + their optical concentrators.

Bottom: Preparation of outer vessel + close-up of an optical concentrator.

Energy Resolution

Energy resolution of a calorimeter where *E* is energy of incoming particle:

$$\frac{\sigma}{E} = \frac{a}{\sqrt{E}} \oplus \frac{b}{E} \oplus c$$

***a*, stochastic term** — Fluctuations in the number of signal generating processes, ie on the number of photo-electrons generated

***b*, noise term** — Noise in readout electronics
'pile-up' due to other particles from other collision events arriving close in time

Energy Resolution

$$\frac{\sigma}{E} = \frac{a}{\sqrt{E}} \oplus \frac{b}{E} \oplus c$$

***c* , constant term**

Imperfections in calorimeter construction (dimension variations)
Non-uniform detector response

Channel to channel intercalibration errors
Fluctuations in longitudinal energy containment

Energy lost in dead material, before or in detector

Crucial to have small constant term for good energy resolution at the highest particle energies

Energy Resolution

$$\frac{\sigma}{E} = \frac{a}{\sqrt{E}} \oplus \frac{b}{E} \oplus c$$ ← added in quadrature !

Consider a physics search for a 2 TeV Z'→ e+e-
Suppose each electron has energy E = 1 TeV = 1000 GeV

In the CMS electromagnetic calorimeter:

Stochastic term, a = 3%	**3% / sqrt E(GeV)**	**~ 0.1%**
Noise term, b = 250 MeV	**0.25 GeV / E (GeV)**	**~ 0.0%**
Constant term, c = 0.5%		**0.5%**

Resultant resolution, σ/E = 0.1% ⊕ 0% ⊕ 0.5% ~ 0.5%
Resolution at high energies dominated by the constant term

Z' mass will be measured to a precision of ~ sqrt(2) * 0.5% ~ 0.7% = 14 GeV

With calorimetry, the resolution, *σ/E,* <u>improves</u> with increasing particle energy

Goal of calorimeter design - find best compromise between the three contributions
- at a price you can afford !

Intrinsic em energy resolution for homogeneous calorimeters

Intrinsic resolution of homogeneous e.m. calorimeters

Energy released in the detector material mainly ionisation and excitation

Mean energy required to **produce a 'visible' scintillation photon** in a crystal **or an electron-ion pair** in a noble liquid Q

Mean number of quanta produced $\langle n \rangle = E_0 / Q$

The intrinsic energy resolution is given by the fluctuations on 'n'

$$\sigma_E / E = \sqrt{n} / n = \sqrt{(Q / E)}$$

Typically obtain $\boldsymbol{\sigma_E / E}$ **1% - 3% / $\sqrt{E}$ (GeV)**

However, in certain cases:

Energy of the incident particle is **only** transferred to making quanta, and to no other energy dissipating processes, for example in Germanium.

Fluctuations much reduced:

$\boldsymbol{\sigma_E / E = \sqrt{(FQ / E)}}$ where F is the 'Fano' factor .

F ~ 0.1 in Ge

Detector resolution in **AGATA** 0.06% (rms) for 1332 keV photons

The AGATA Germanium detector

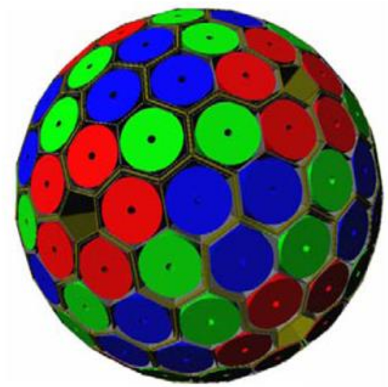

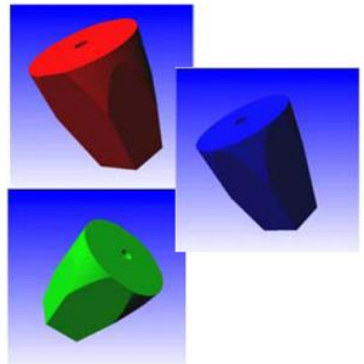

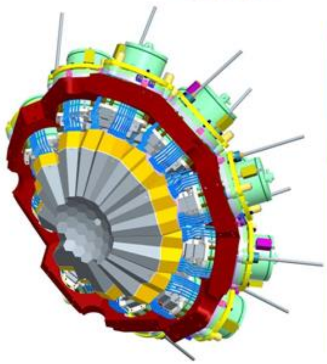

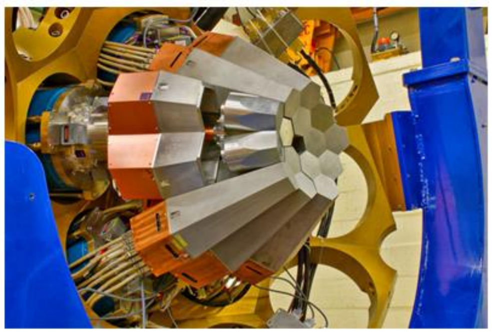

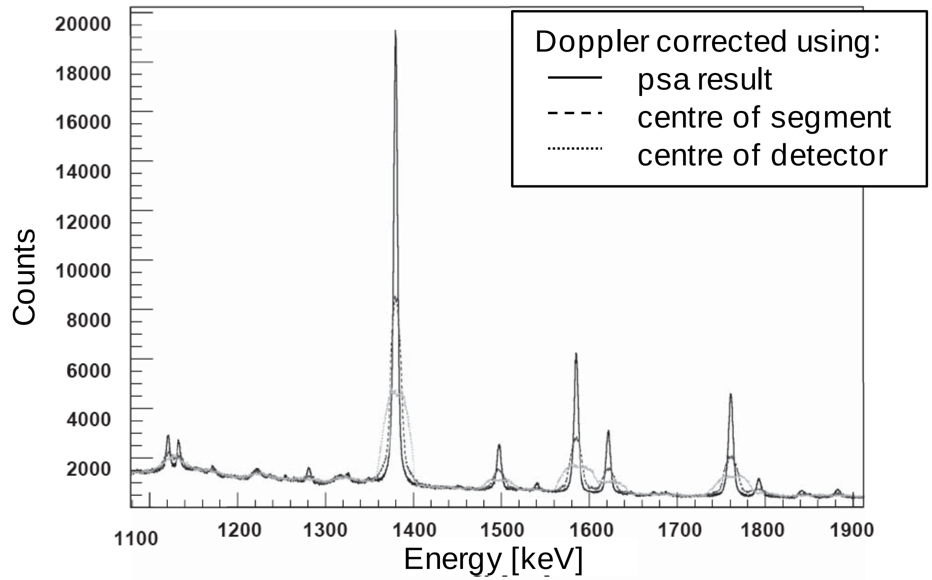

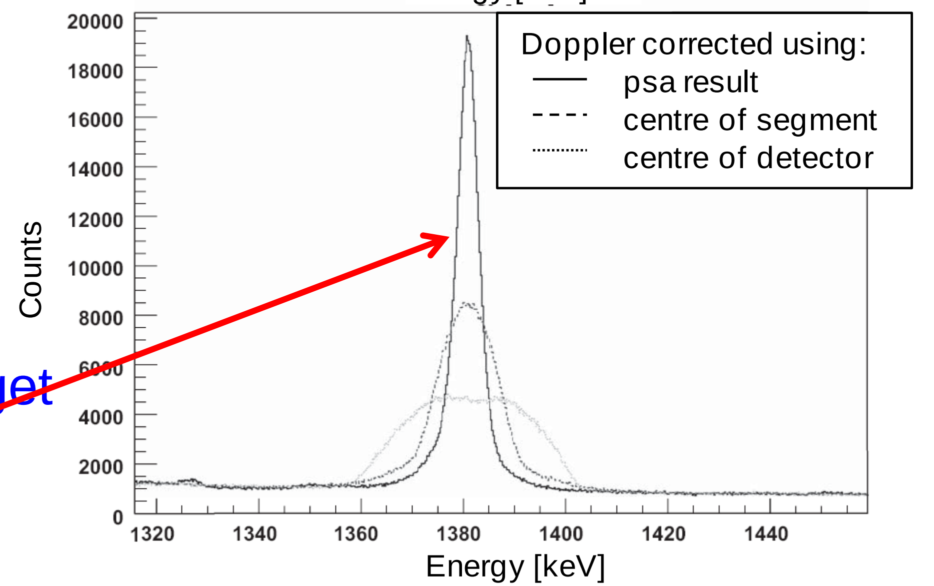

Experiment with excited nucleii from a target

1382 keV line width 4.8 keV (fwhm)

Resolution 0.15%

Resolution 0.06% with a source

Energy resolution - the CMS $PbWO_4$ crystal calorimeter

Scintillation emission only small fraction of energy loss in crystal, so Fano factor, $F \sim 1$

However – get fluctuations in the avalanche process in the Avalanche Photodiodes (APDs) used for the photo-detection
- gives rise to an **excess noise factor** for the gain of the device

$F \sim 2$ for the crystal + APD combination

$N_{pe} \sim 4500$ photo-electrons released by APD, per GeV of deposited energy

Stochastic term $\quad a_{pe} = \sqrt{F / N_{pe}} = \sqrt{(2 / 4500)} = 2.1\%$

This assumes total lateral shower containment

In practice energy summed over limited 3x3 or 5x5 arrays of crystals, to minimise added noise

Expect $a_{leak} = 2\%$ from an energy sum over a 3x3 array of crystals

Expect a stochastic term of $\quad a = a_{pe} \oplus a_{leak} = 2.9\%$
Measured value $\quad 2.8\%$

Energy resolution

CMS ECAL , 3x3 array of $PbWO_4$ crystals
Test beam electrons

a , stochastic term = 2.83%
c , constant term = 0.26%

$$\frac{\sigma}{E} = \frac{a}{\sqrt{E}} \oplus \frac{b}{E} \oplus c$$

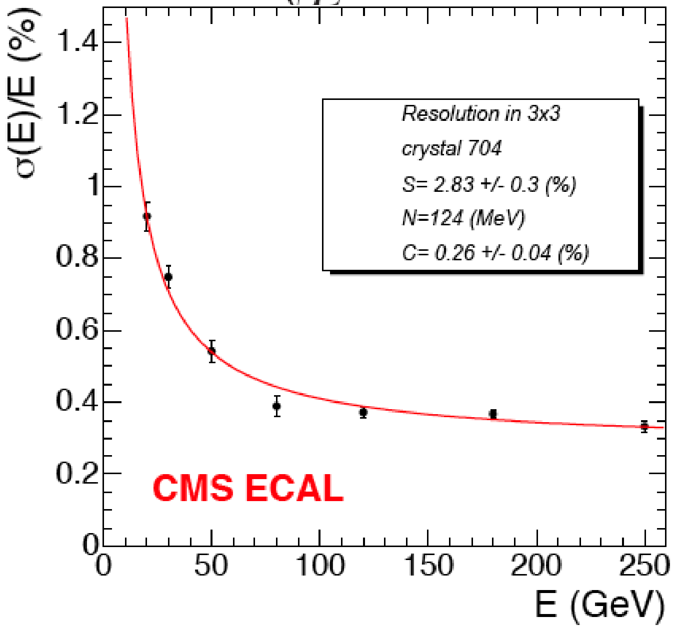

Borexino
Photoelectron yield ~500 per MeV

Expect √500 / 500 = 4.4%
Measured ~5% at 1 MeV

Prior to installation: modules taken to test beams at CERN and elsewhere

In situ in CMS: trigger, record and use known resonances to calibrate the crystals

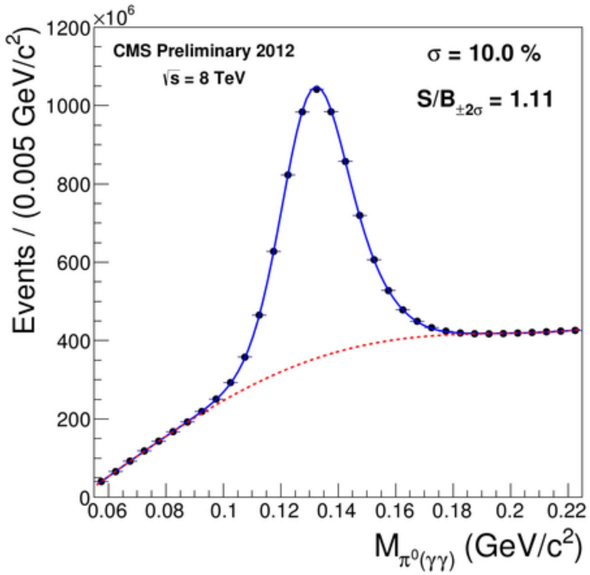

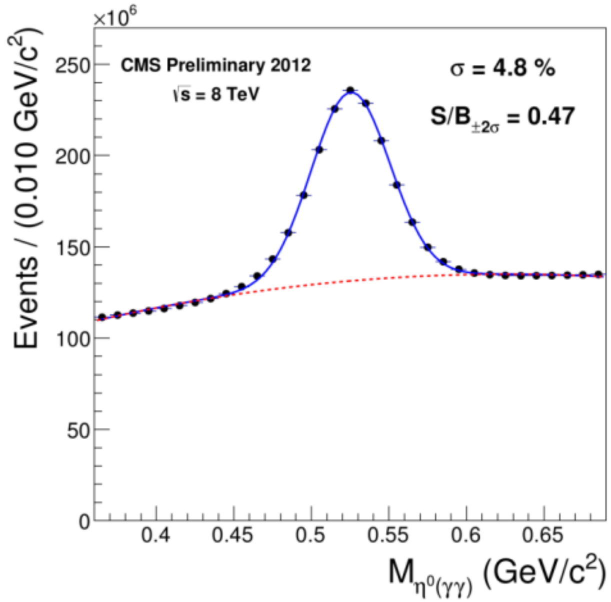

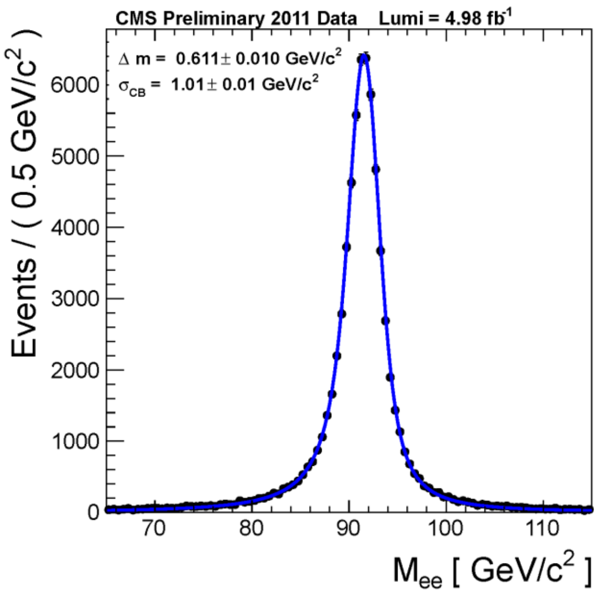

$\pi^0 \rightarrow \gamma\gamma$

$\eta \rightarrow \gamma\gamma$

$Z \rightarrow ee$
peak at 91 GeV
width of Gaussian 1.01 GeV
Crucial input for resolution estimates for $H \rightarrow \gamma\gamma$ at 125 GeV

In situ in CMS also use:

W decays, $W \rightarrow e^{\pm} \upsilon$

Electron energy, E, measured in the ECAL
Electron momentum, p, measured in the Tracker
Optimize the E/p distributions (E/p = 1 ideally)

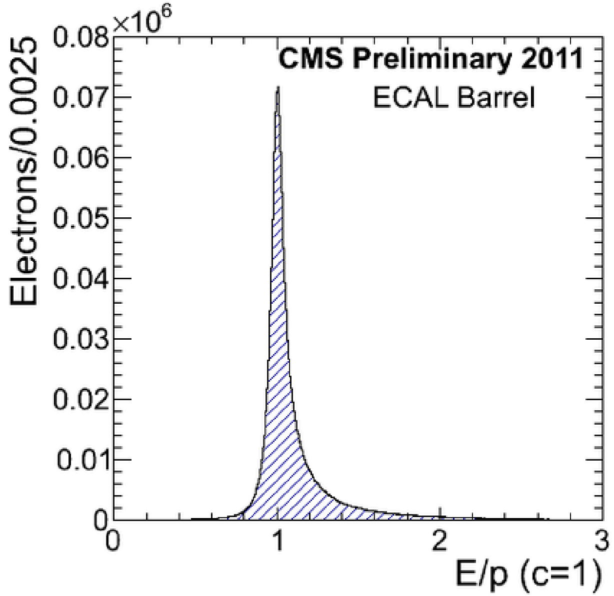

Phi symmetry (gives quick initial values)
The transverse energy flow, summed over many "minimum bias" collisions, should be the same towards any phi angle

Use this symmetry to calibrate rings of individual crystals sitting at the same pseudorapidity

Getting excellent energy resolution – in a real detector !!

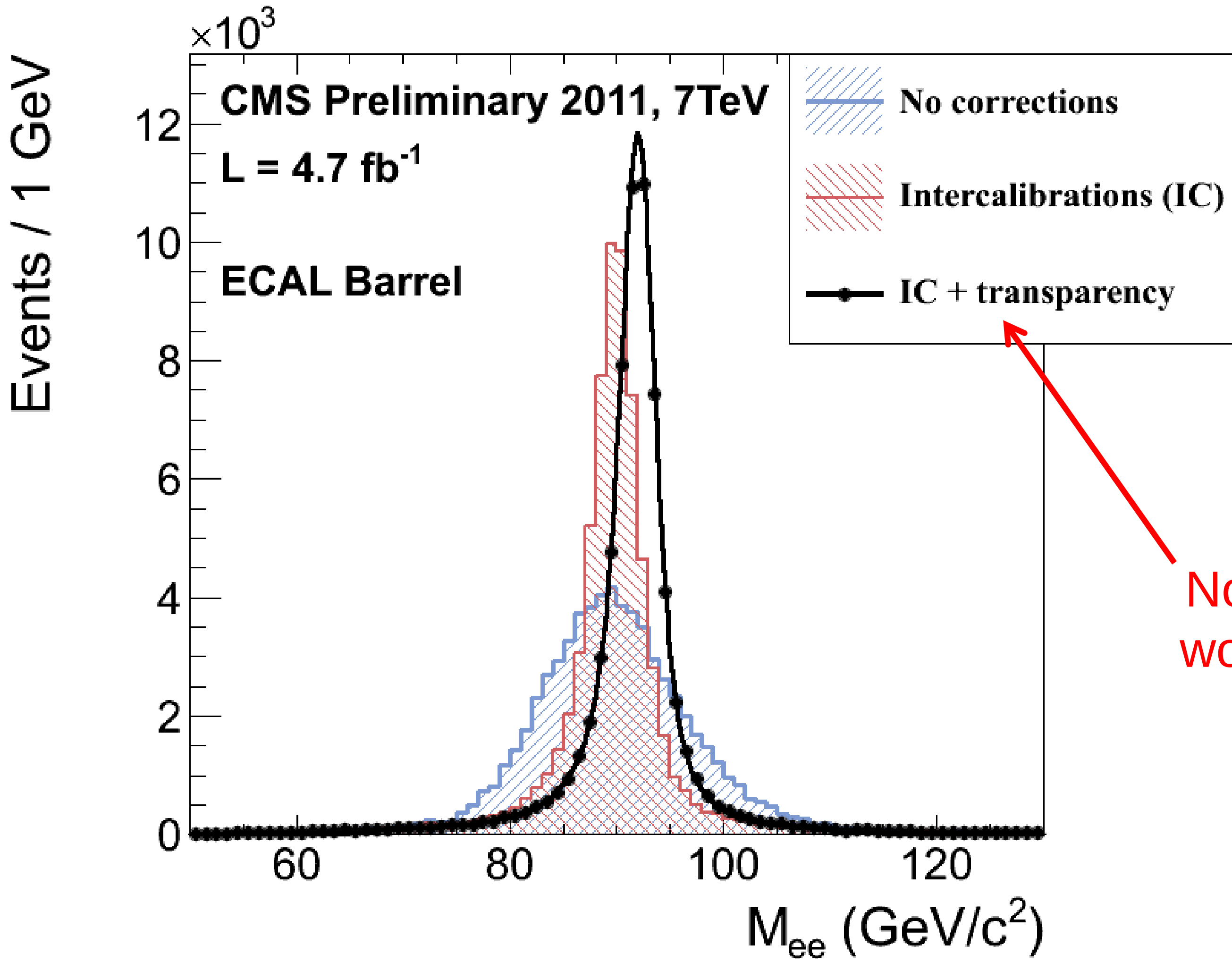

Note the crucial work needed for the various corrections

Instrumental resolution of 1.01 GeV from Z -> ee decays in the CMS ECAL Barrel

Intrinsic resolution of sampling electromagnetic calorimeters

Sampling fluctuations arise due to variations in the number of charged particles crossing the active layers

$n_{charged} \propto E_o / t$ (t = thickness of each absorber layer)

If each sampling is independent $\sigma_{samp} / E = 1/\sqrt{n_{charged}} \propto \sqrt{(t / E)}$

Need ~100 sampling layers to compete with homogeneous devices.

Typically $\sigma_{samp}/E \sim 10\%/\sqrt{E}$

Intrinsic resolution of sampling electromagnetic calorimeters

ATLAS stochastic term ~10%

constant term 0.3%

Thickness of the 1-2 mm thick absorber sheets controlled to 6.6 µm to achieve a constant term of 0.3%

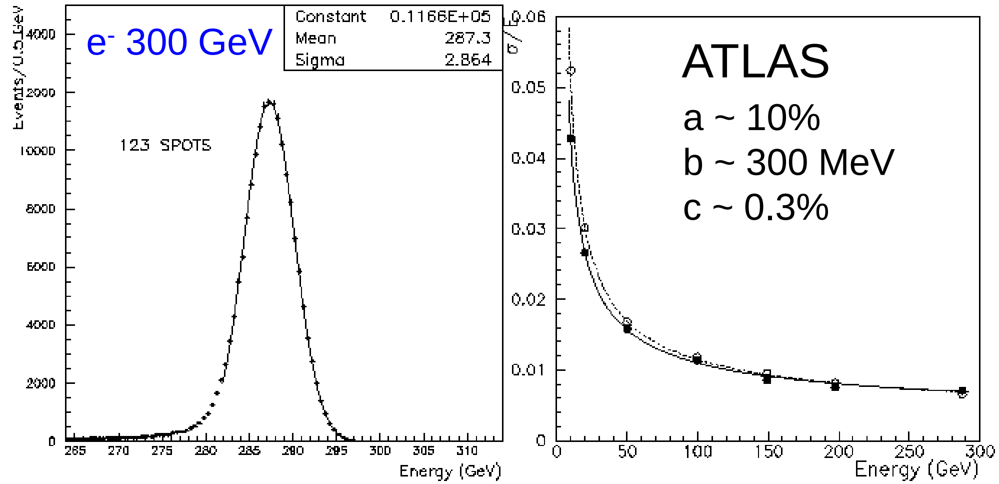

Also: ATLAS spatial resolution ~5mm / √E (GeV)

LHCb stochastic term 9.4%

constant term 0.83%

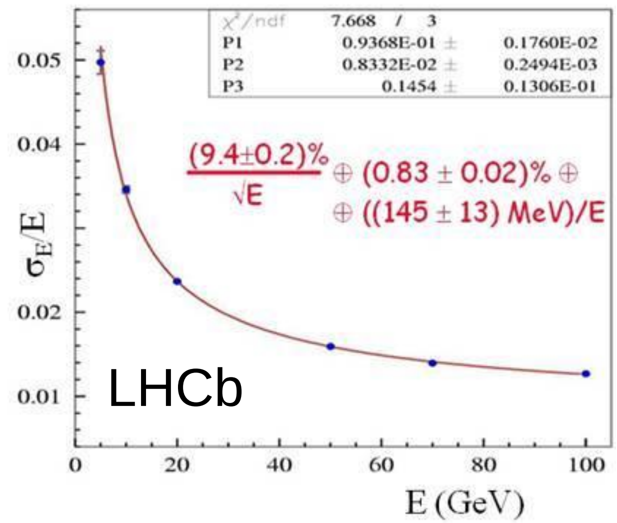

Hadronic Calorimetry

Hadronic cascades **much more complex** than e.m. cascades

Shower development determined by the mean free path, λ_I , between inelastic collisions

The nuclear interaction length is given by $\lambda_I = A / (N_A.\sigma_{inel})$, $\sigma_{inel} \approx \sigma_0 A^{0.7}$ $\sigma_0 \approx 35\, mb$

Expect $\sigma_I \propto A^{2/3}$ and thus $\lambda_I \propto A^{1/3}$.

In practice, $\lambda_I \sim 35\, A^{1/3} = 16.7$ cm in iron

High energy hadrons interact with nuclei producing secondary particles, mostly $\pi^{\pm}$ and π^{o}

Lateral spread of shower from transverse energy of secondaries, <p_T> ~ 350 MeV/c

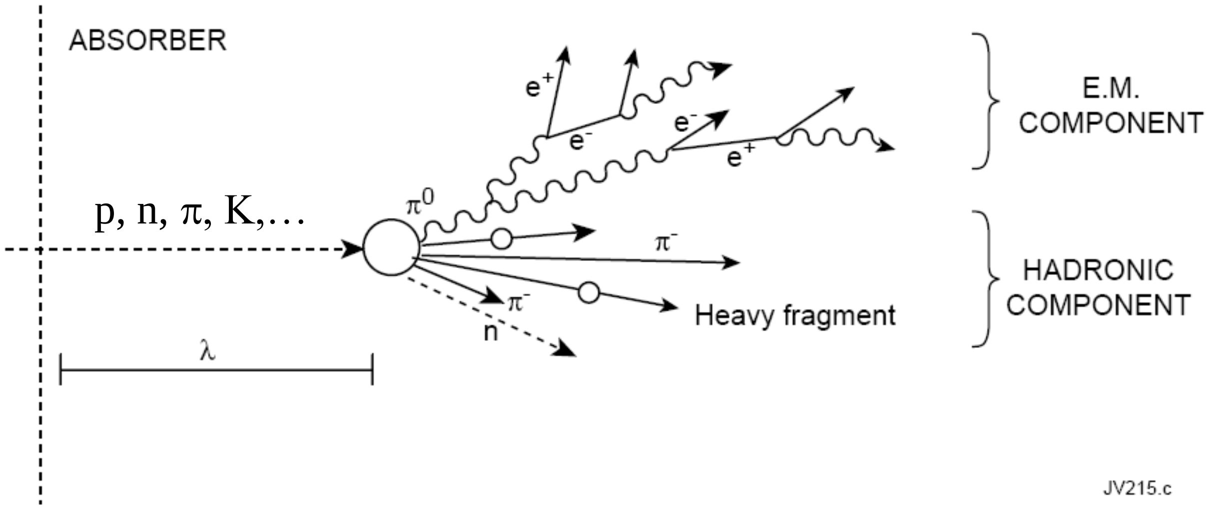

Hadronic Cascades

For a collision with a nucleus:
Multiplicity of secondary particles $\propto \ln(E)$

~ 1/3 of the pions produced are neutral pions, π^0
$n(\pi^0) \sim \ln E\ (GeV) - 4.6$

For a 100 GeV incoming hadron, $n(\pi^0) \approx 18$

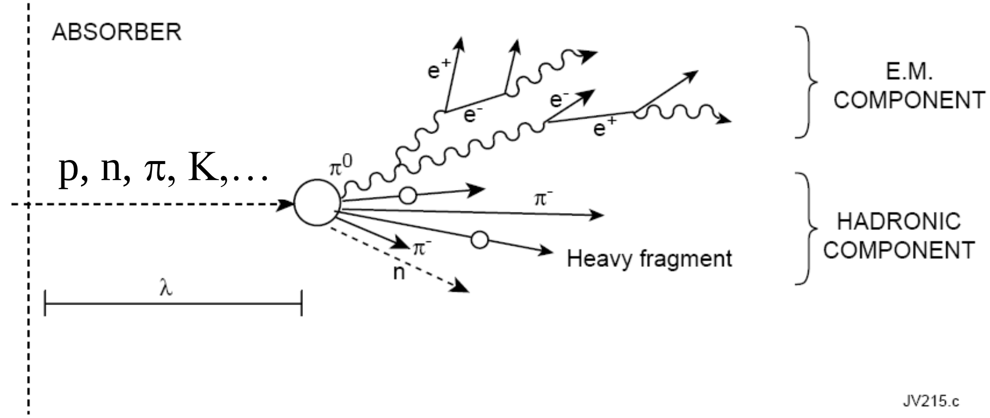

The neutral pions quickly decay to two electromagnetic particles (2 photons)
$\pi^0 \rightarrow \gamma\gamma$ in $\sim 10^{-16}$ s

Thus hadronic cascades have two distinct components:
hadronic (largely π^+, π^-, heavy fragments, excited nuclei) and electromagnetic ($\gamma\gamma$)

This gives rise to a much more complex cascade development which limits the ultimate resolution possible for hadronic calorimetry

Simulations of hadron showers

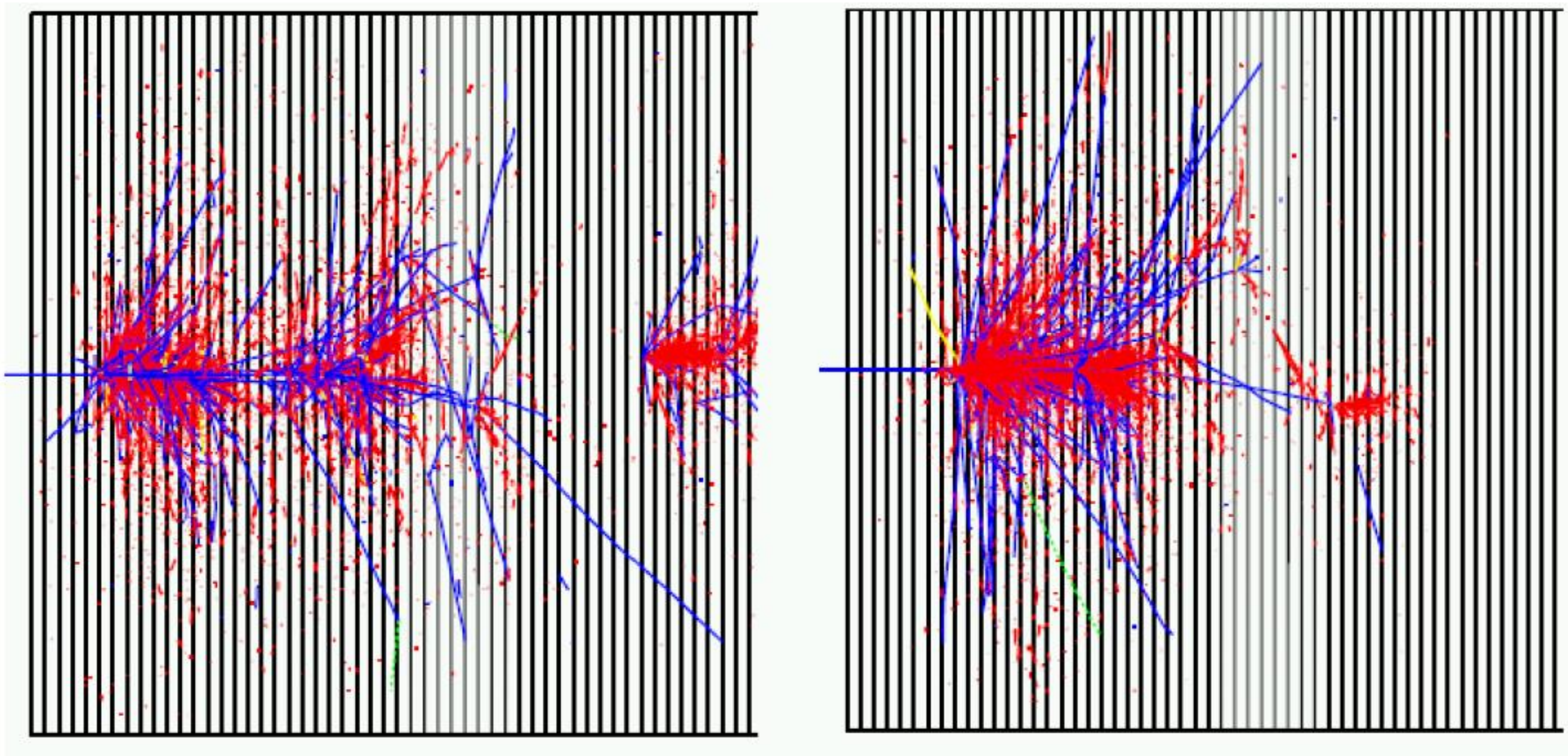

Red - e.m. component   Blue – charged hadrons

Unlike electromagnetic showers, hadron showers do not show a uniform deposition of energy throughout the detector medium

Hadronic Cascades

Hadronic longitudinal shower development

The e.m. component more pronounced at the start of the cascade than the hadronic component

Shower profile characterised by a peak close to the first interaction, Then, an exponential fall off with scale λ_I

$$t_{\max}(\lambda_I) \approx 0.2 \ln E[GeV] + 0.7$$

$$t_{95\%}(cm) \approx a \ln E + b$$

To contain 95% of the energy in Iron:

a = 9.4, b=39. For E =100 GeV, $t_{95\%} \approx$ 80 cm

For adequate containment, need ~10 λ_I

In Iron, need 1.67 m. In Copper need 1.35 m

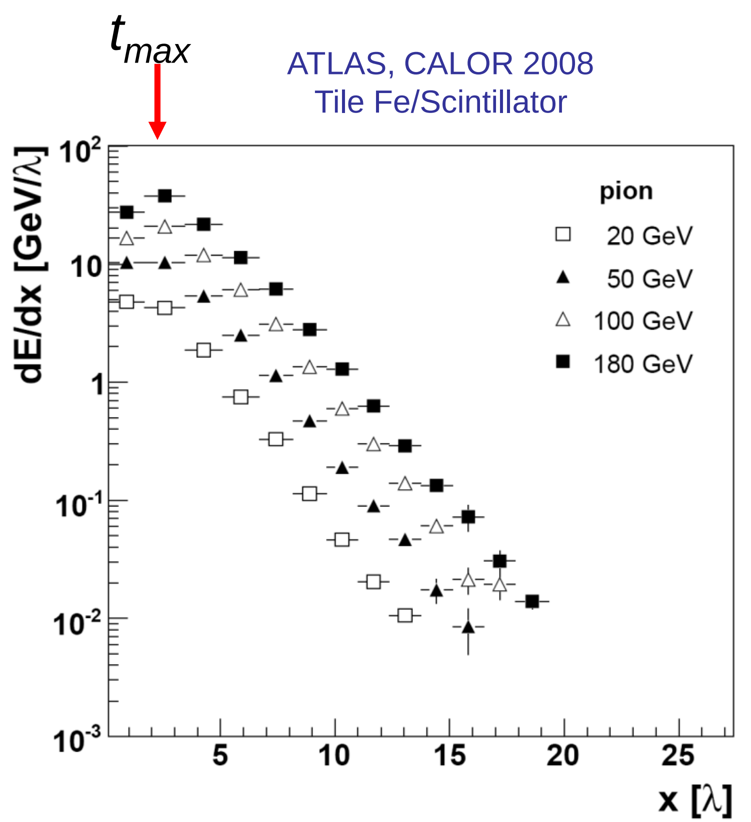

Longitudinal profile of pion induced showers at various energies

Hadronic lateral shower development

The shower consists of core + halo

95% containment : cylinder of radius λ_I = 16.7 cm in iron

Compare to a radius of **2.19 cm** for an em cascade in $PbWO_4$

Comparison – electromagnetic showers vs hadronic showers

Electromagnetic versus hadronic scale for calorimetry

$X_0 \sim 180\, A / Z^2 \quad << \quad \lambda_I \sim 35\, A^{1/3}$

E.M shower size in PbWO4 **23 cm deep x 2.19 cm radius**

Hadron shower size in Iron **80 cm deep x 16.7 cm radius**

Hadron cascades much longer and broader than electromagnetic cascades

Hadron calorimeters much larger than em calorimeters

Detectors for Hadronic Calorimetry

Hadron Sampling Calorimeters

CMS Hadron calorimeter at the LHC   Brass absorber preparation

Workers in Murmansk sitting on brass casings of **decommissioned shells of the Russian Northern Fleet**

Explosives previously removed!

Casings melted in St Petersburg and turned into raw brass plates

Machined in Minsk and mounted to become absorber plates for the CMS Endcap Hadron Calorimeter

CMS Hadron sampling calorimetry

The CMS HCAL being inserted into the solenoid

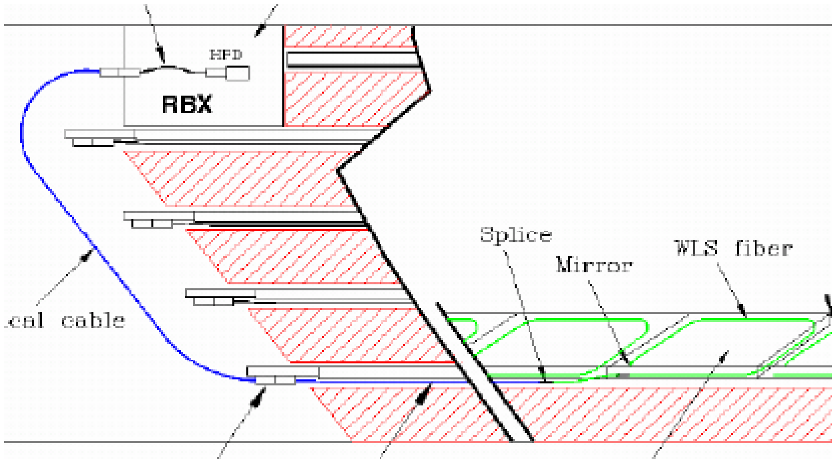

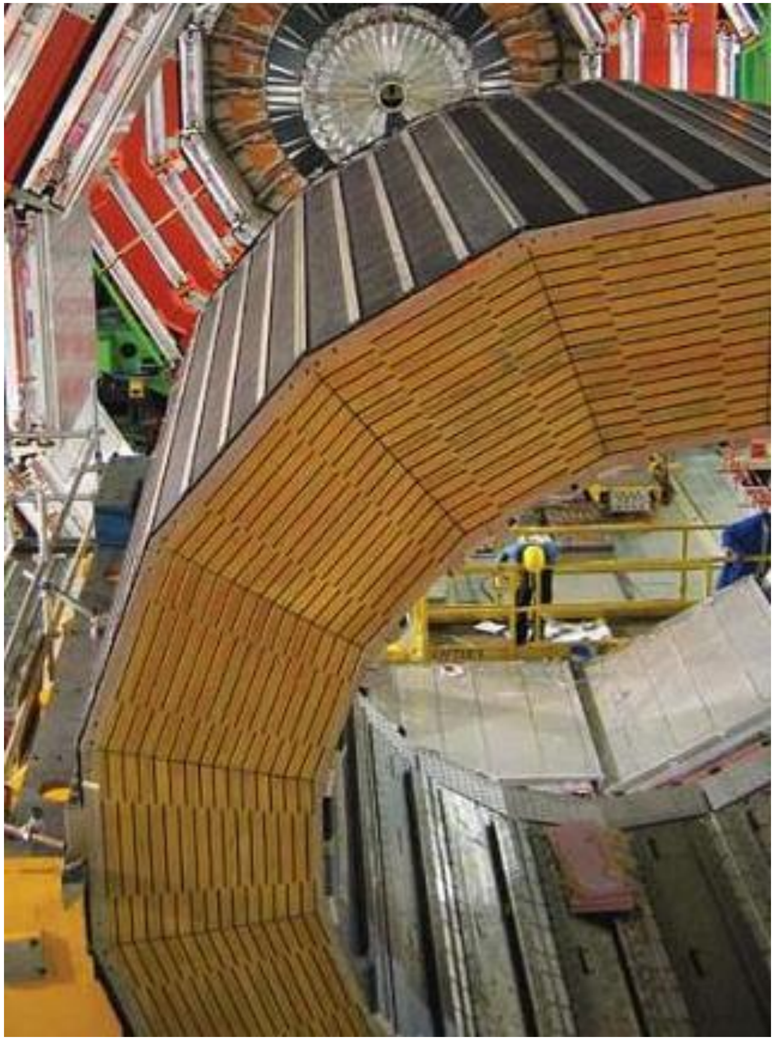

Light produced in the scintillators is transported through optical fibres to Hybrid Photo Diode (HPD) detectors

CMS HCAL – fibre readout

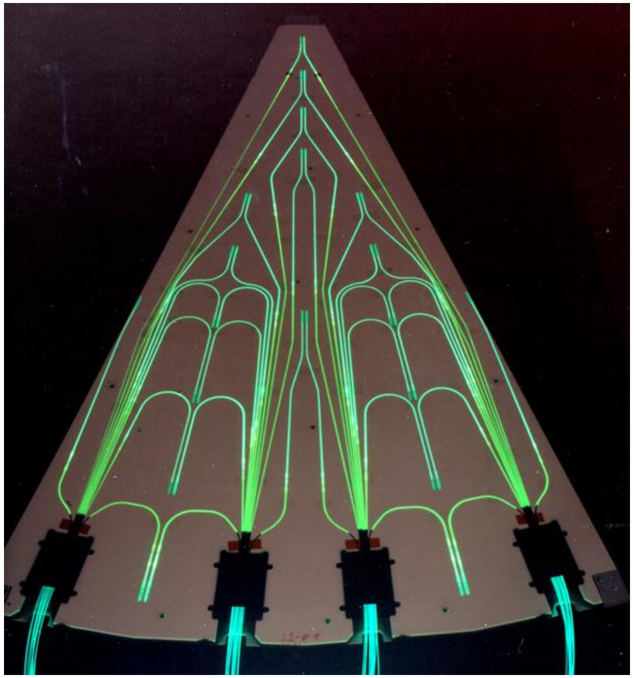

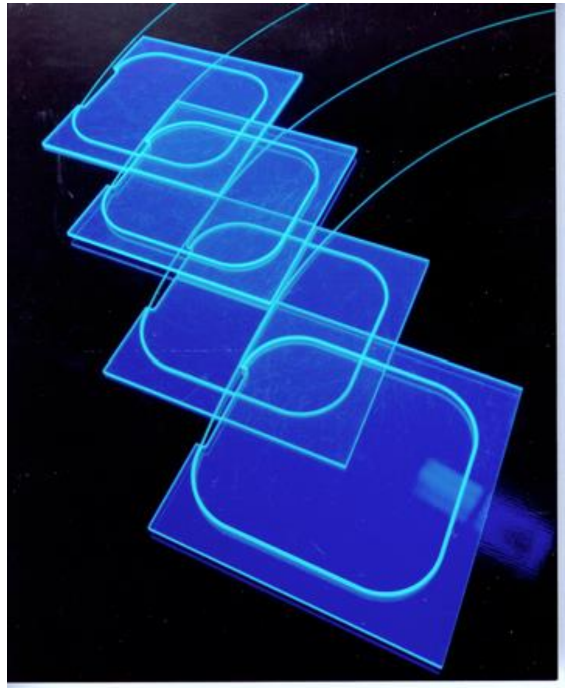

Scintillator tile inspection

Light emission from the scintillator tiles blue-violet, λ = 410-425 nm.

This light is absorbed by wavelength shifting fibers which fluoresce in the green, λ = 490 nm.

The green light is conveyed via clear fiber waveguides to connectors at the ends of the scintillator megatiles.

CMS Hadron sampling calorimetry

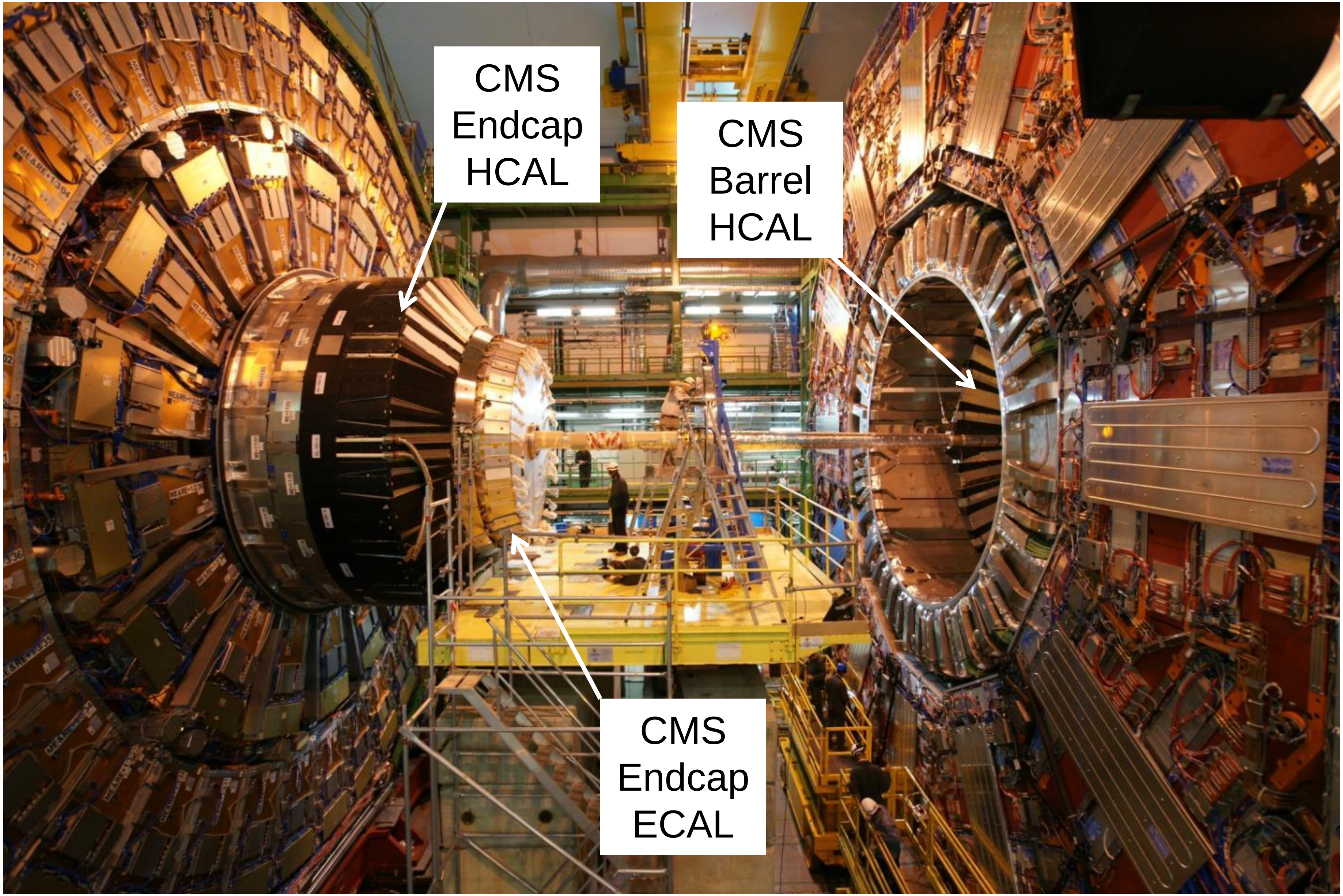

Hadron calorimetry resolution

Strongly affected by the energy lost as 'invisible energy':

- nuclear excitation followed by delayed photons (by up to to ~1μsec, so usually undetected)
- soft neutons
- nuclear binding energy

Fluctuations in the 'invisible energy' play an important part in the degradation of the intrinsic energy resolution

Hadron energy dissipation in Pb

Nuclear break-up (invisible) 42%
Charged particle ionisation 43%
Neutrons with T_N ~ 1 MeV 12%
Photons with E_γ ~ 1 MeV 3%

Further degradation

If the calorimeter responds differently as a function of energy to the em component of the cascade ($\pi^0 \rightarrow \gamma\gamma$)

F_{π^o} ~ *1/3* at low energies
F_{π^o} ~ *a log(E)* (the em part increases or 'freezes out' with energy)

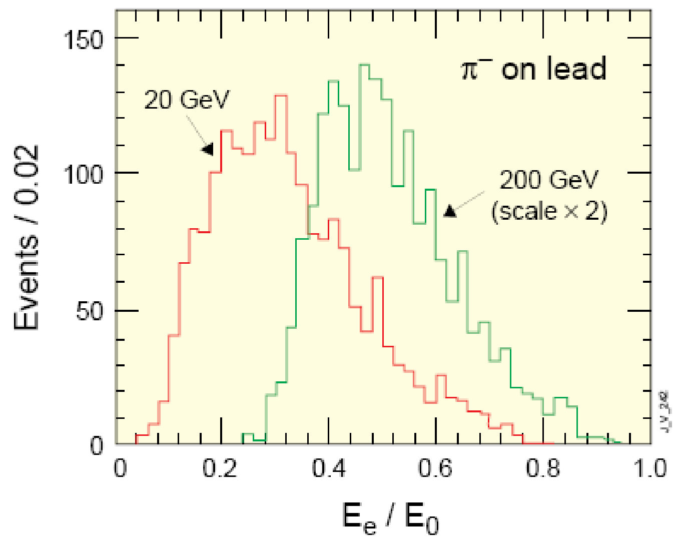

EM fraction for 20 GeV and 200 GeV pions on lead

Energy resolution of hadronic calorimeters

In general, the hadronic component of a hadron shower produces a smaller signal than the em component

so $e/h > 1$

Consequences for $e/h \neq 1$

- response with energy is non-linear
- fluctuations of the em component of the cascade, F_{π°, worsen the energy resolution, σ_E/E

The fluctuations are non-Gaussian, consequently

- σ_E/E improves more slowly with energy than for an electromagnetic calorimeter
- More as 1/ E than $1/\sqrt{E}$

'Compensating' sampling hadron calorimeters seek to restore $e/h = 1$ to achieve better resolution and linearity (see backup slide)

Single hadron energy resolution in CMS at the LHC

Compensated hadron calorimetry & high precision em calorimetry are usually incompatible

In CMS, hadron measurement combines **HCAL** (Brass/scint) and ECAL($PbWO_4$) data

Effectively a hadron calorimeter divided in depth into two compartments

Neither compartment is 'compensating':
e/h ~ 1.6 for ECAL
e/h ~ 1.4 for HCAL

Hadron energy resolution is degraded and response is energy-dependent

Stochastic term a = 120%
Constant term c = 5%

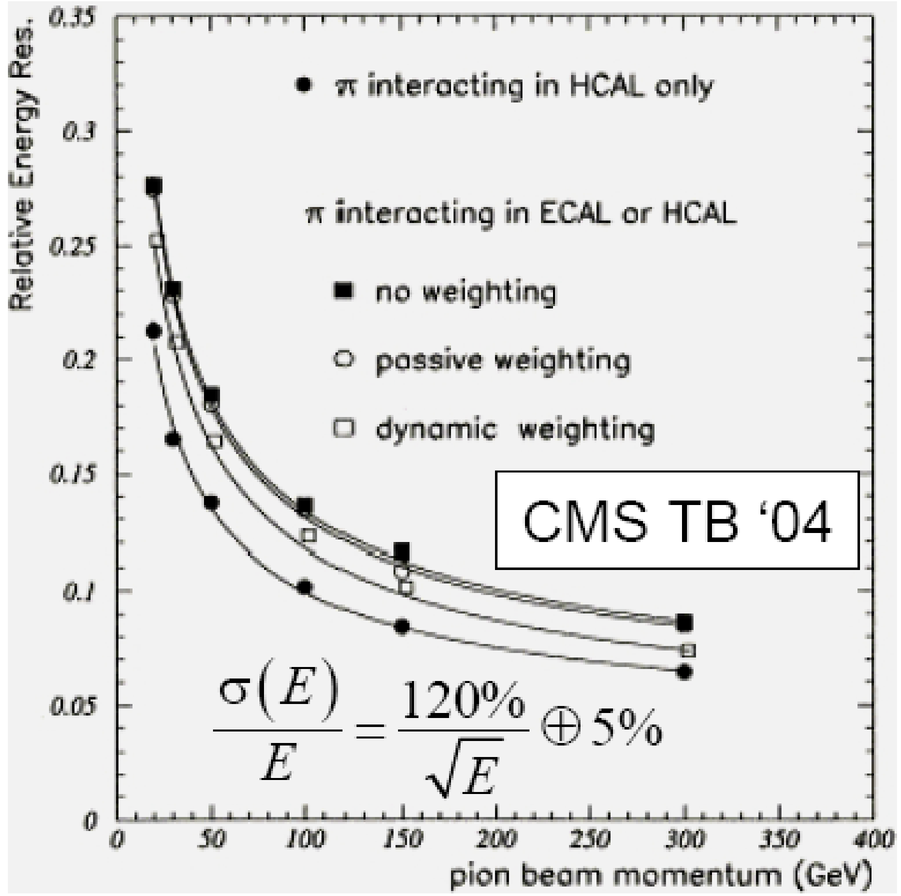

CMS energy resolution for single pions up to 300GeV

Jets and Particle Flow

At colliders, hadron calorimeters serve primarily to measure jets and missing E_T

Single hadron response gives an indication of the level to be expected for jet energy resolution

Make combined use of

- Tracker information
- fine grained information from the ECAL and HCAL detectors

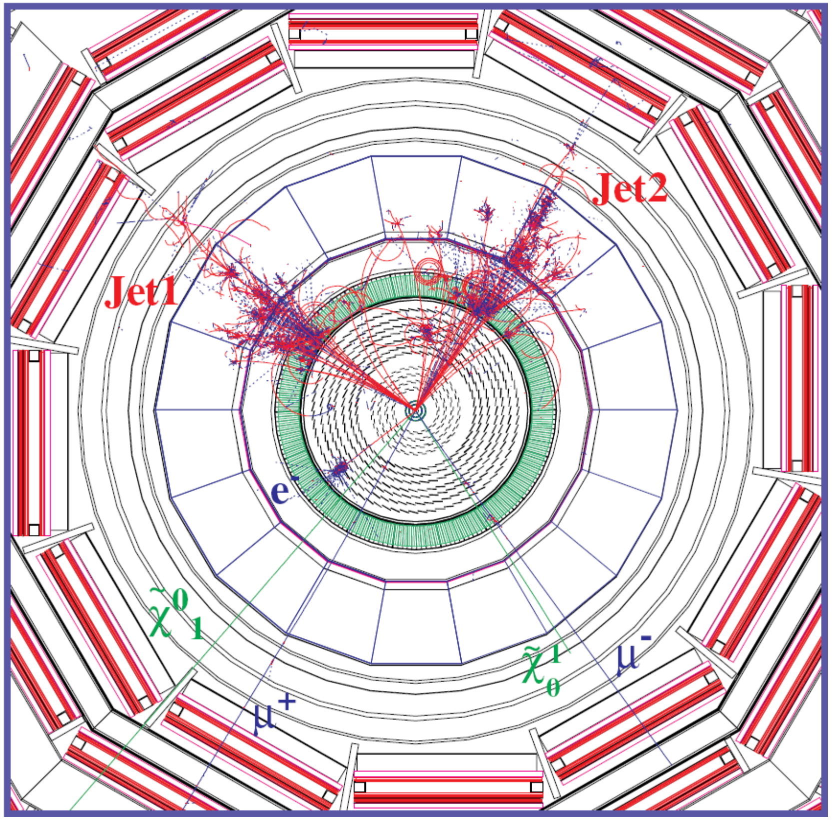

Jets from a simulated event in CMS

Traditional approach

Components of jet energy only measured in ECAL and HCAL

In a typical jet 65% of jet energy in charged hadrons
25% in photons (mainly from $\pi^o \rightarrow \gamma\gamma$)
10% in neutral hadrons

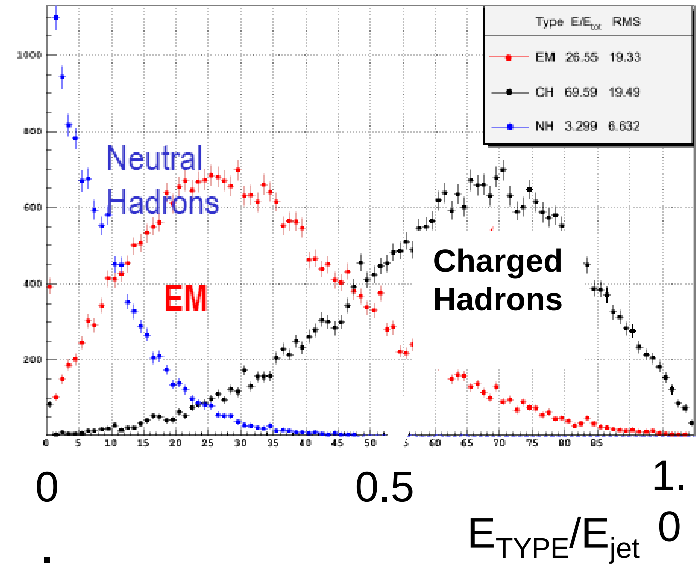

Particle Flow Calorimetry

- Charged particles measured with tracker, when better
- Photons measured in ECAL
- Leaves only neutral hadrons in HCAL (+ECAL)

Only 10% of the jet energy (the neutral hadrons) left to be measured in the poorer resolution HCAL

Dramatic improvements for overall jet energy resolution

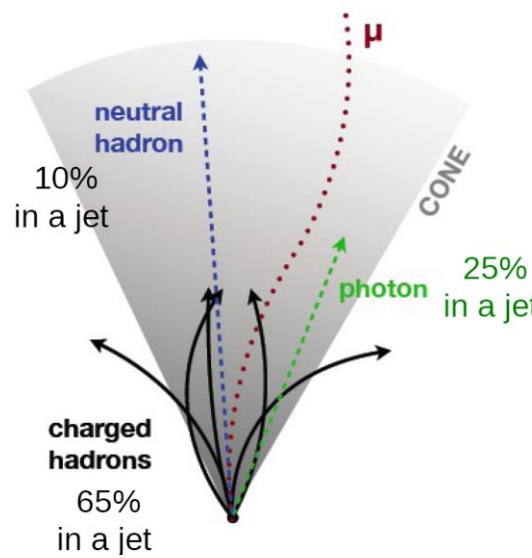

Momenta of particles inside a jet

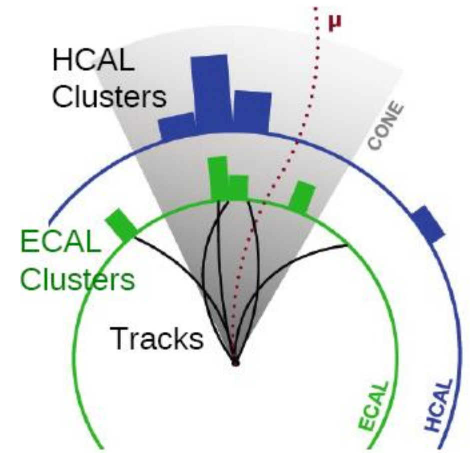

Consider a quark/gluon jet, total p_T = 500 GeV/c
Average p_T carried by the stable constituent particles of the jet **~ 10 GeV**

Jets with p_T < 100 GeV, constituents O (GeV)

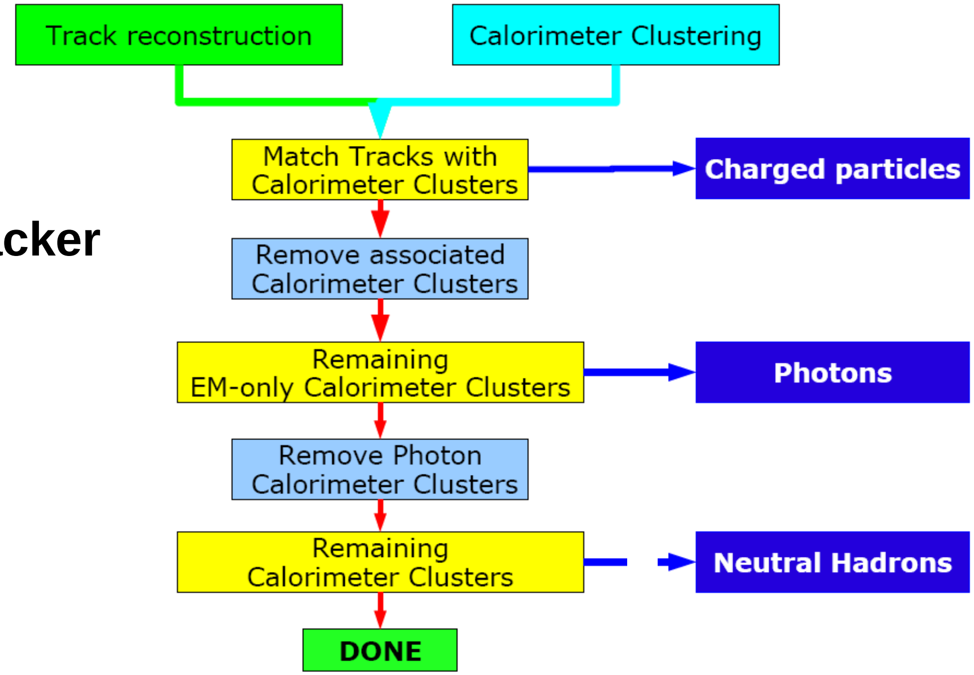

For charged particles with momenta O (GeV) better to use momentum resolution of the Tracker

Particle Flow versus Calorimetry alone

- CMS - large central magnetic field of 4T
- Very good charged particle track momentum resolution
- Good separation of charged particle energy deposits from others in the calorimeters
- Good separation from other tracks

Large improvement in jet resolution at low P_T using the combined resolution of the Calorimetry and Tracking systems

Simulated QCD-multijet events, CMS barrel section: $|\eta| < 1.5$

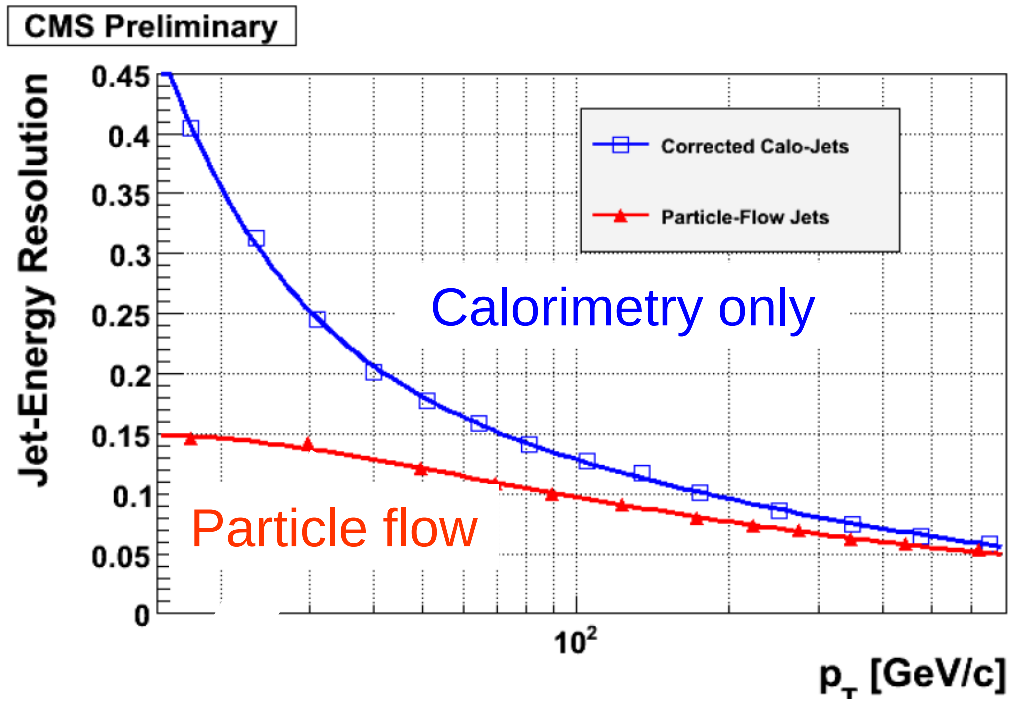

Jet energy resolution as a function of P_T

Higgs and Calorimetry

Event recorded with the CMS detector in 2012

Characteristic of Higgs boson decay to 2 photons

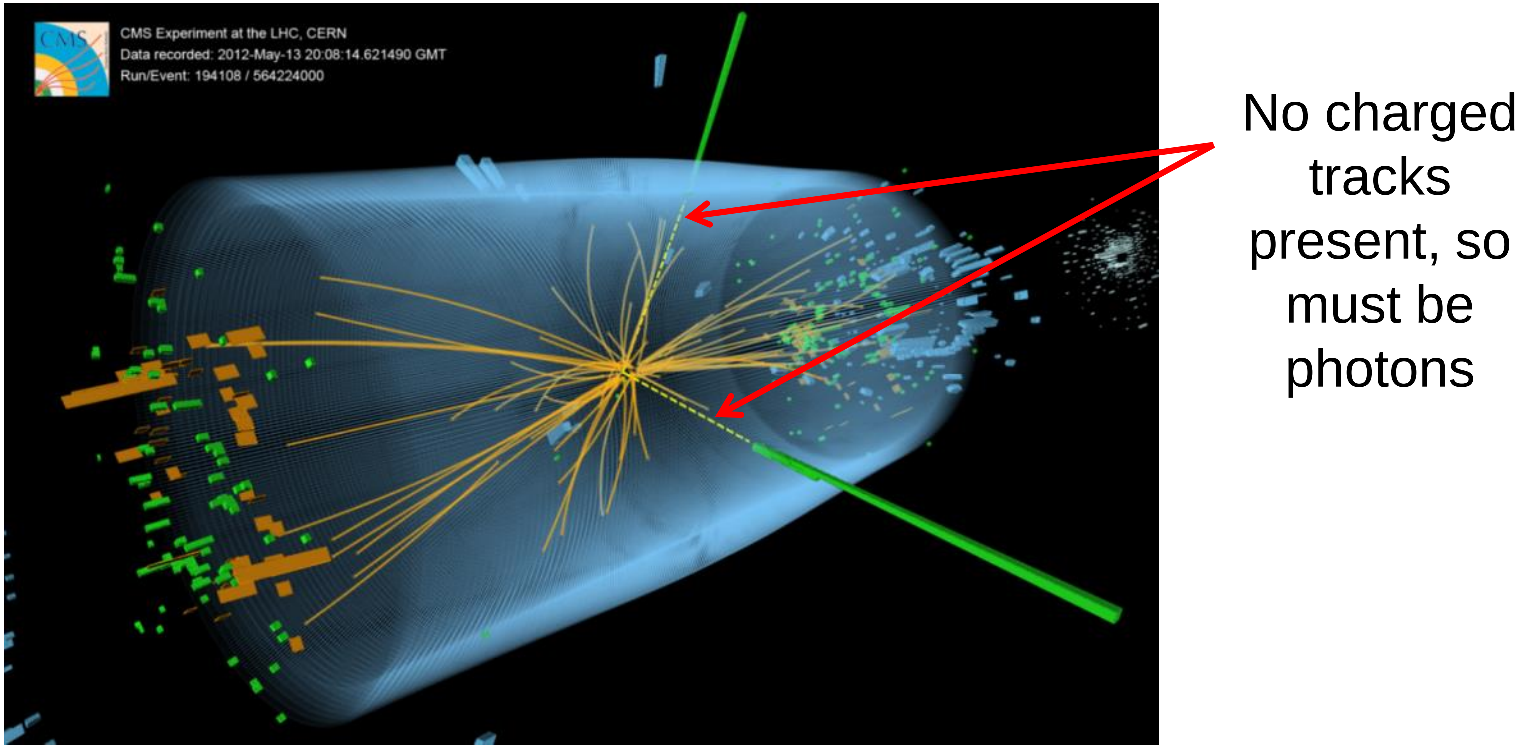

EM calorimetry	Hadronic calorimeter	Tracker	Muon detector
E.m. energy proportional to green tower heights	**Hadron energy proportional to orange tower heights**	**Charged tracks Orange curves**	**Muon detector hits Blue towers**

Can **YOU** calculate the **Effective mass** for the 2 high energy photons in the event??

Photon 1

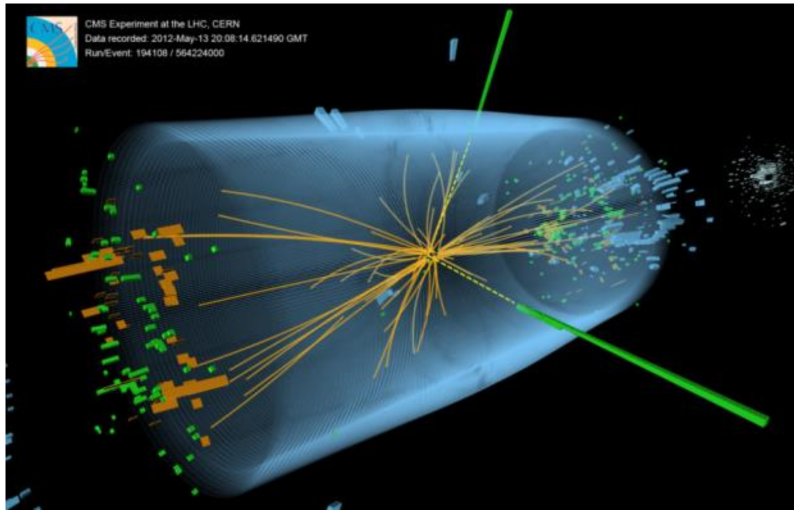

Photon 2

	ECAL Energy (GeV)	Angle Phi ** (radians)	Pseudo-rapidity ** (η)
Photon 1	90.0264	0.719	0.0623
Photon 2	62.3762	2.800	-0.811

** see definitions in next slide

You can also ask Professor Moretti for his estimate !

CMS Event – angle definitions

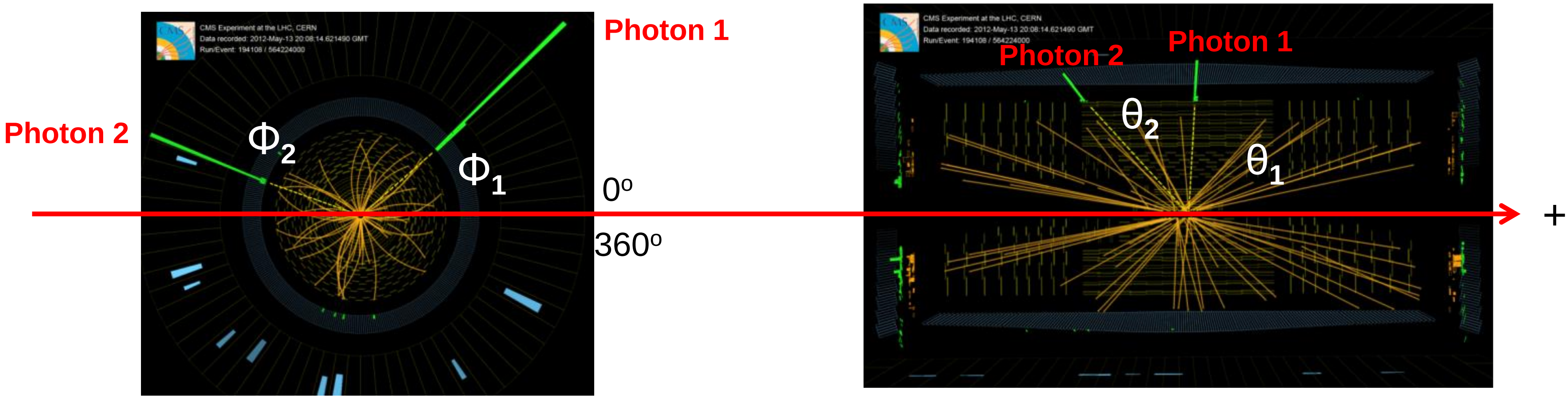

Transverse view

Angle of the photons in the r-phi plane, Φ_1 and φ_2

Φ_1 = **0.719 radians**
Φ_2 = **2.800 radians**

Longitudinal view

Angle of the photons wrt the +ve direction of the beam axis, θ_1 and θ_2

θ related to pseudo-rapidity (η) by

$$\eta = - \ln [\tan (\theta/2)]$$

η_1 = **0.0623**
η_2 = **- 0.8110**

The crowning glory of CMS (and ATLAS) calorimetry!

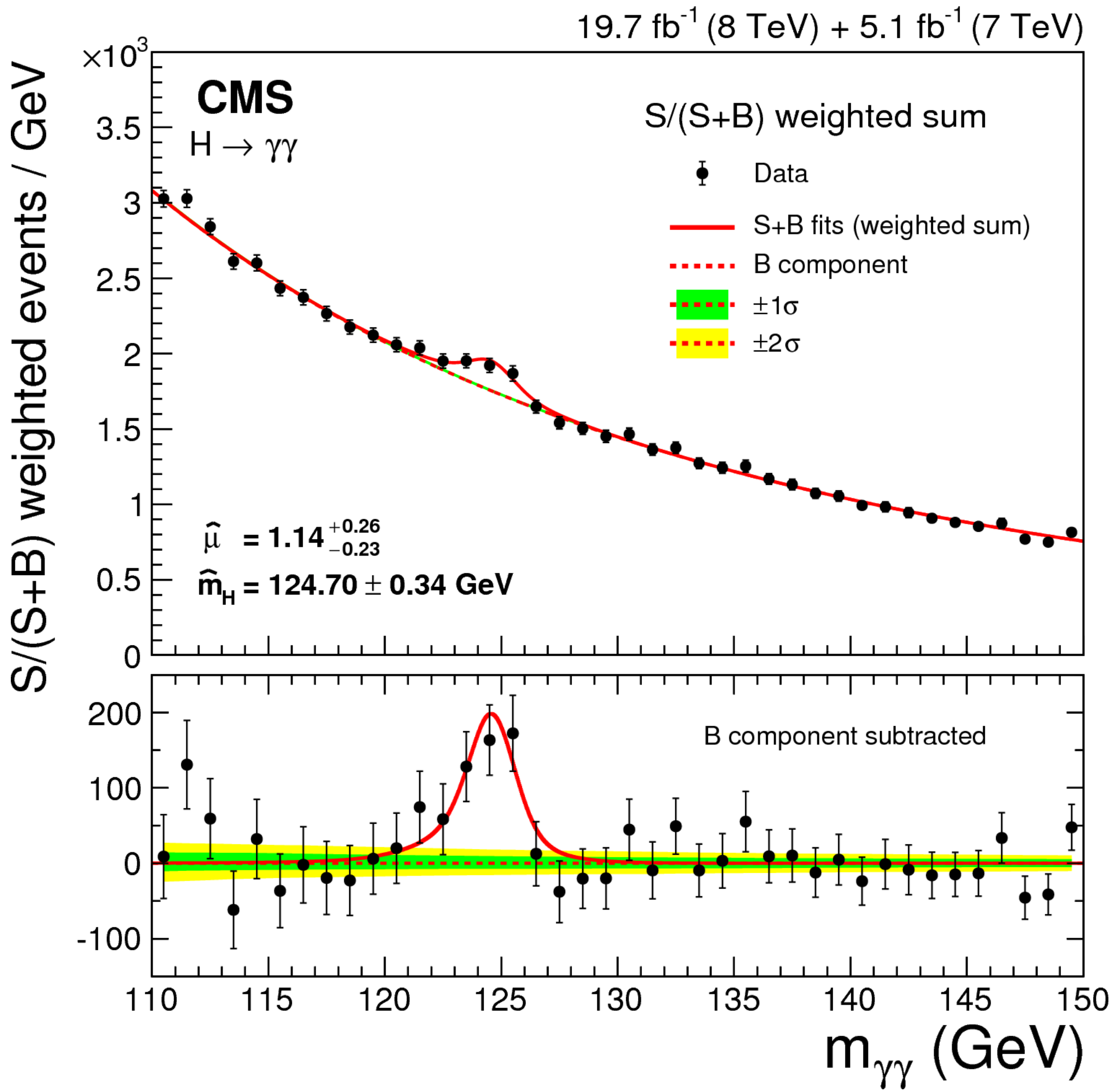

Summary

Calorimetry a key detector technique for particle physics

In this talk, calorimtery for photons/electrons from ~1 MeV, to O(50 GeV) for Z decays, to O(1 TeV) for jets

Calorimeters playing a crucial role for physics at the LHC, eg $H \rightarrow \gamma\gamma$, $Z' \rightarrow ee$, SUSY (missing E_T)

Calorimeters indispensible for neutrino and missing E_T physics

Wide variety of technologies available. Calorimeter design is dictated by physics goals, experimental constraints and cost. Compromises necessary.

References:

Electromagnetic Calorimetry, Brown and Cockerill, NIM-A 666 (2012) 47–79
Calorimetry for particle physics, Fabian and Gianotti, Rev Mod Phys, 75, 1243 (2003)
Calorimetry, Energy measurement in particle physics, Wigmans, OUP (2000)

Backups

Future directions in Calorimetry

The International Linear Collider (ILC)

Use Particle Flow, aided by finely segmented calorimetry

Very high transverse segmentation
ECAL ~1x1 cm^2 SiW cells – CALICE
HCAL ~3x3 cm^2 Steel/scintillator

High longitudinal sampling
30 layers ECAL and 40 layers HCAL

CALICE prototype
1.4/2.8/4.2 mm thick W plates ($30X_0$)
Interleaved with Silicon wafers
Read out at level of 1x1 cm^2 pads

Resolution for electrons
Stochastic term a ~17%
Constant term c ~ 1.1%

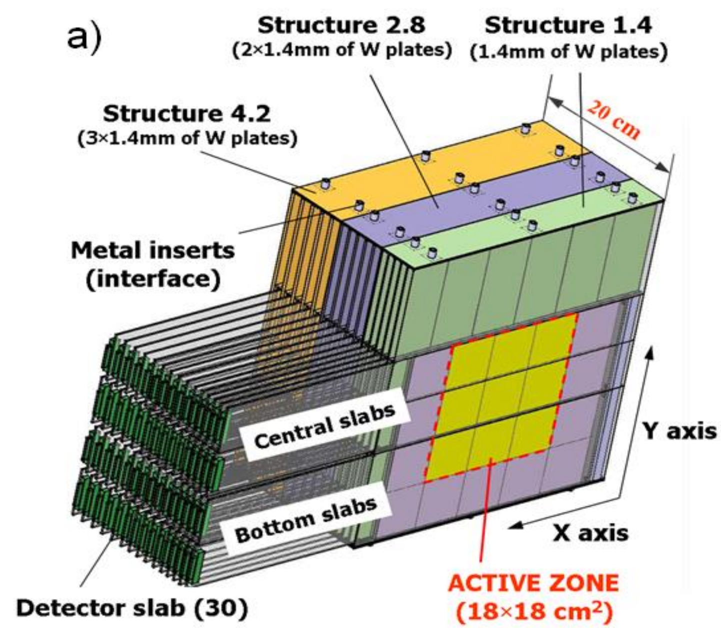

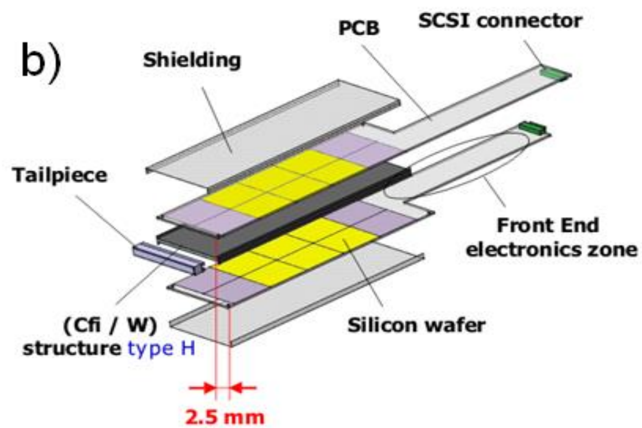

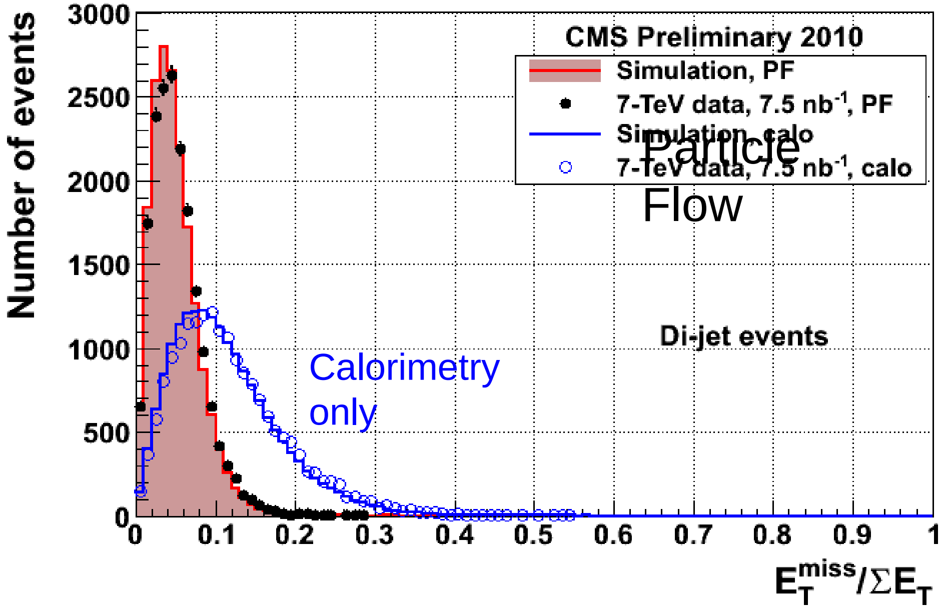

Missing E_T normalised to the total transverse energy for Di-jet events in CMS

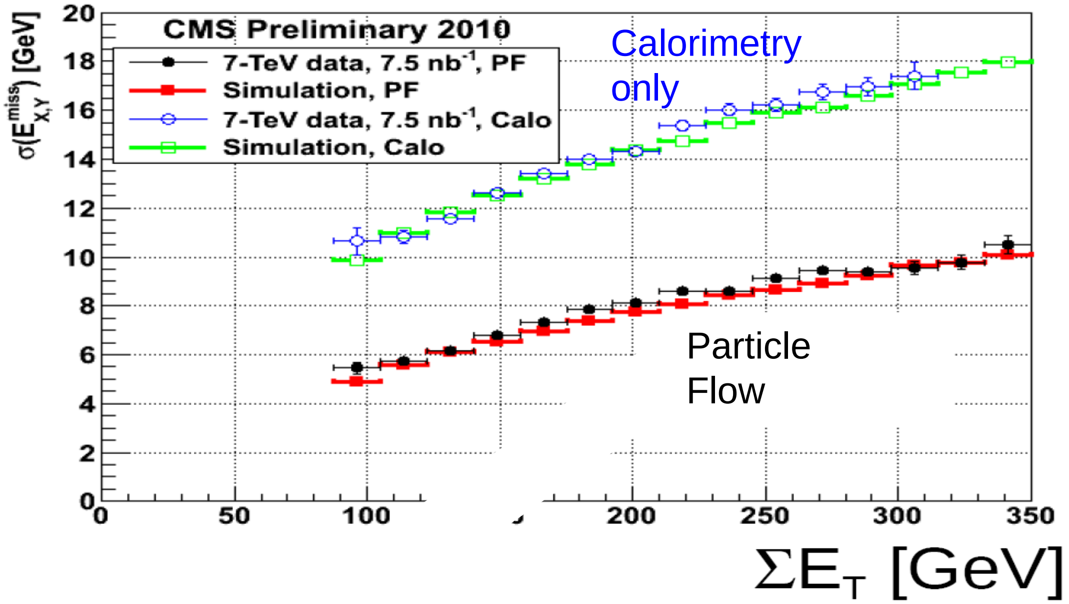

Missing E_T resolution for Di-jet events

CMS missing E_T resolution < 10 GeV over whole ΣE_T range up to 350GeV
Factor 2 improvement on calorimetry by using Particle Flow technique

Energy resolution of hadronic calorimeters

Consequences for $e/h \neq 1$

- response with energy is non-linear
- fluctuations on F_{π° contribute to σ_E/E

Since the fluctuations are non-Gaussian,

- σ_E/E scales more weakly than $1/\sqrt{E}$ *, more as* $1/E$

Deviations from $e/h = 1$ also contribute to the constant term

'Compensating' sampling hadron calorimeters

Retrieve $e/h = 1$ by compensating for the loss of invisible energy, several approaches:

- Weighting energy samples with depth
- Use large elastic cross section for MeV neutrons scattering off hydrogen in the organic scintillator
- Use ^{238}U as absorber. ^{238}U fission is exothermic. Release of additional neutrons

Neutrons liberate recoil protons in the active material

Ionising protons contribute directly to the signal

Tune absorber/scintillator thicknesses for $e/h = 1$

Example Zeus: ^{238}U plates (3.3mm)/scintillator plates (2.6mm), total depth 2m, $e/h = 1$

Stochastic term $0.35/\sqrt{E(\text{GeV})}$

Additional degradation to resolution, calorimeter imperfections :

Inter-calibration errors, response non-uniformity (laterally and in depth), energy leakage, cracks

ALICE at the LHC – scintillating $PbWO_4$ crystals

Avalanche photo diode readout

Some of the 17,920 $PbWO_4$ crystals for ALICE (PHOS)

Homogeneous calorimeters

Three main types: Scintillating crystals Glass blocks (Cerenkov radiation) Noble liquids

Crystals	NaI(Tl)	CsI(Tl)	CsI	BGO	$PbWO_4$
Density (g/cm^3)	3.67	4.53	4.53	7.13	8.28
X_0 (cm)	2.59	1.85	1.85	1.12	0.89
R_M (cm)	4.5	3.8	3.8	2.4	2.2
Decay time (ns)	250	1000	10	300	5
slow component			36		15
Emission peak (nm)	410	565	305	410	440
slow component			480		
Light yield γ/MeV	4×10^4	5×10^4	4×10^4	8×10^3	1.5×10^2
Photoelectron yield (relative to NaI)	1	0.4	0.1	0.15	0.01
Rad. hardness (Gy)	1	10	10^3	1	10^5

Lead glass, SF-6
OPAL at LEP
X_o = 1.69cm,
ρ = 5.2 g/cm^3

Barbar @PEPII 10ms inter'n rate good light yield, good S/N

KTeV at Tevatron, High rate, Good resolution

L3@LEP, 25μs bunch crossing, Low rad'n dose

CMS at LHC 25ns bunch crossing, high radiation dose
ALICE
PANDA

The Power of Calorimetry
A high energy DiJet event in CMS

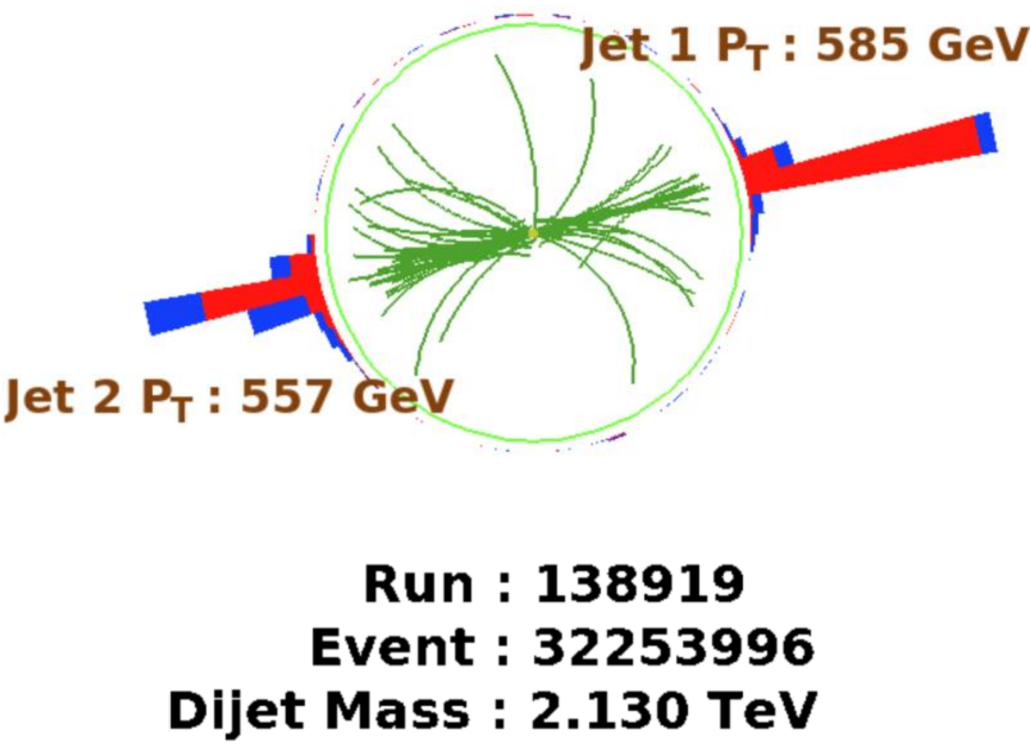

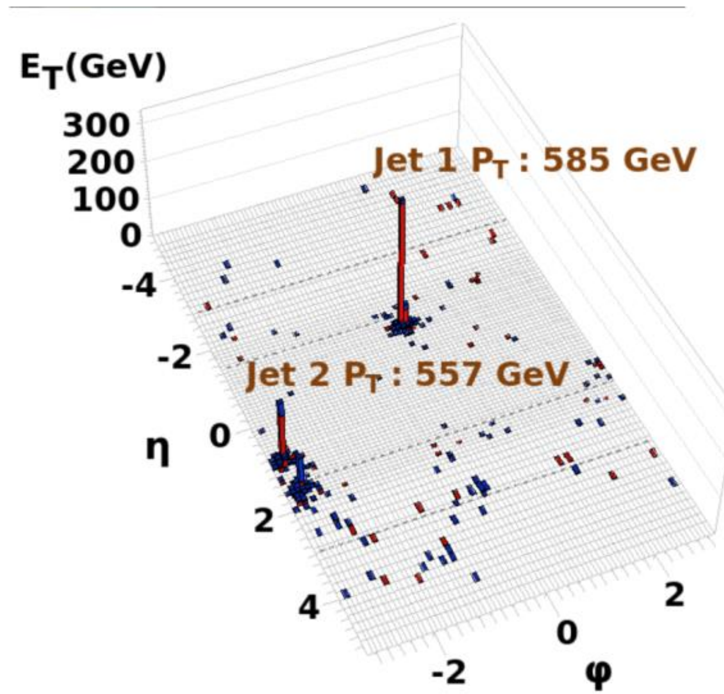

Calorimeter energy deposits on η x φ map
ECAL red, HCAL blue

A high mass dijet event in the first 120nb^{-1} of data, at 2.13 TeV taken in CMS with pp collisions at 7 TeV, July 2010

Extra info – em shower depth

How many X_0 to adequately contain an em shower?

Rule of thumb

RMS spread in shower leakage at the back ~ 0.5 * average leakage at the back

CMS - keep rms spread < 0.3% => leakage < 0.65% => crystals $25X_0$ (23cm) long

Other relations

$<t_{95\%}> \sim t_{max} + 0.08Z + 9.6$

$<t_{98\%}> \sim 2.5\, t_{max}$

$<t_{98\%}> \sim t_{max} + 4\, \lambda_{att}$

Tail of cascade - photons of a few MeV ~ at the min in the mass attenuation coefficient

$\lambda_{att} \sim 3.4X_0$ ~ photon mean free path.

λ_{att} is associated with the exponential decrease of the shower after t_{max}

Extra info – em profile Pb versus Cu

Comment, em longitudinal profile, Pb versus Cu:

The coulomb field in Pb, Z=82 with E_c = 7.3 MeV means that bremstrahlung dominates over ionisation to much lower shower particle energies than for example in Cu, Z=29 with E_c = 20.2 MeV

As a consequence the depth (in X_o) of a shower proceeds further in Pb than in Cu.

Homogeneous liquid Kr electromagnetic calorimeters

NA48 Liquid Krypton Ionisation chamber (T = 120K)

No metal absorbers: quasi homogeneous

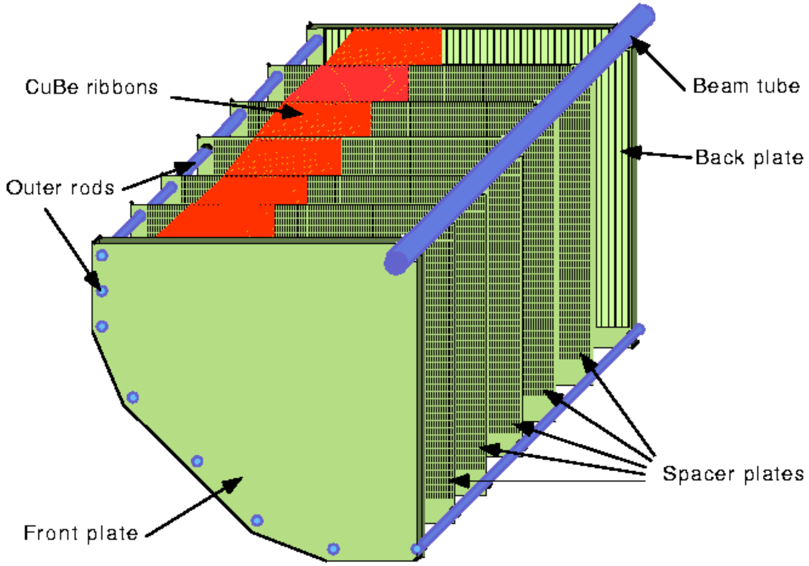

NA48 Liquid Krypton
2cmx2cm cells
X_0 = 4.7cm
125cm length ($27X_0$)
ρ = 5.5cm

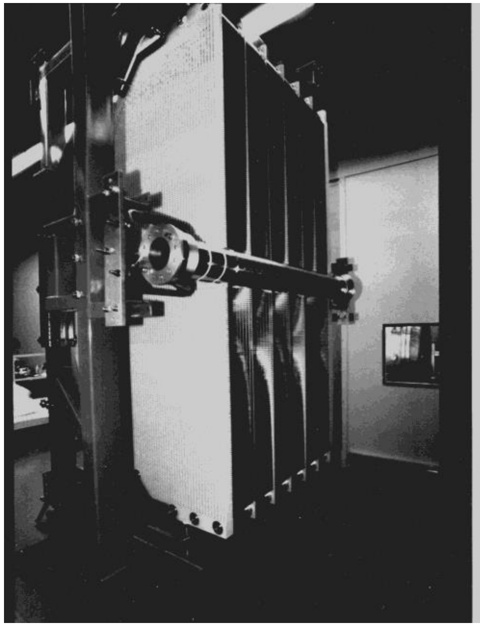

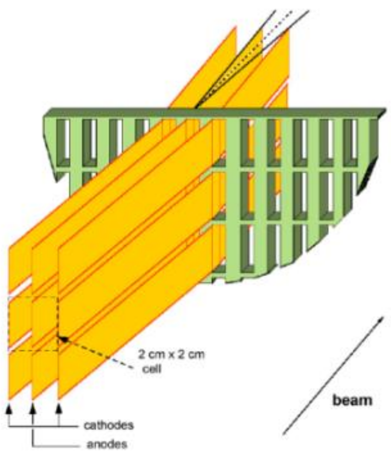

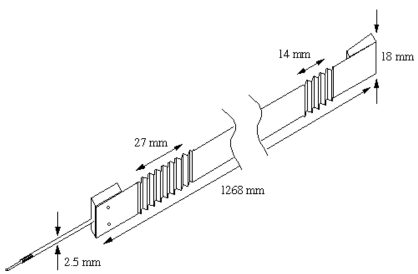

Cu-Be ribbon electrode

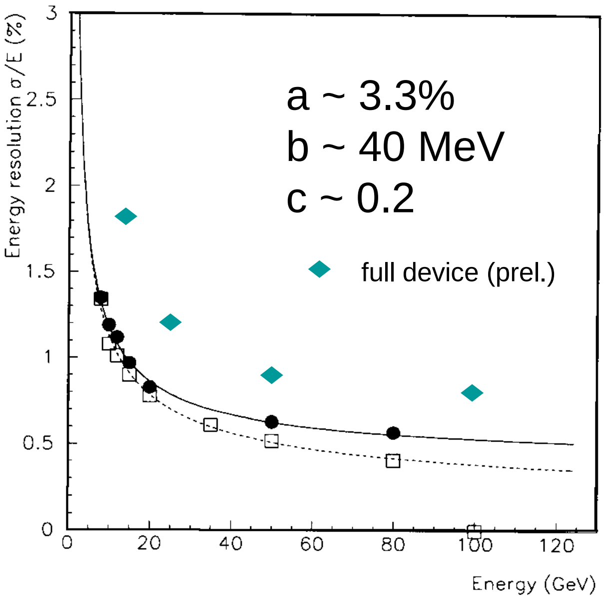

CMS $PbWO_4$ - photodetectors

Barrel

Avalanche photodiodes(APD)

Two 5x5 mm^2 APDs/crystal

Gain 50

QE ~75%

Temperature dependence -2.4%/^{O}C

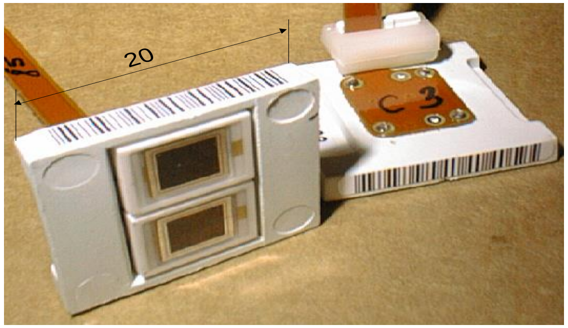

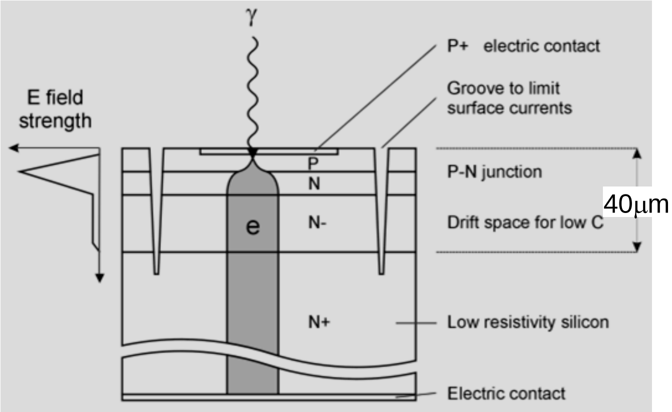

Endcaps

Vacuum phototriodes(VPT)

More radiation resistant than Si diodes

- UV glass window
- Active area ~ 280 mm^2/crystal
- Gain 8 -10 (B=4T)
- Q.E. ~20% at 420nm

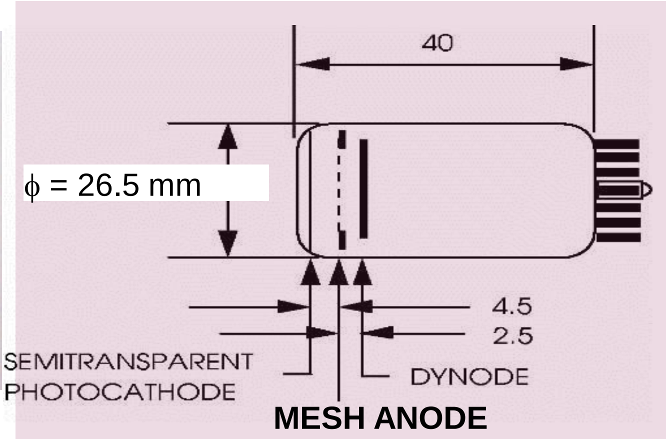

$PbWO_4$ - CMS ECAL energy resolution

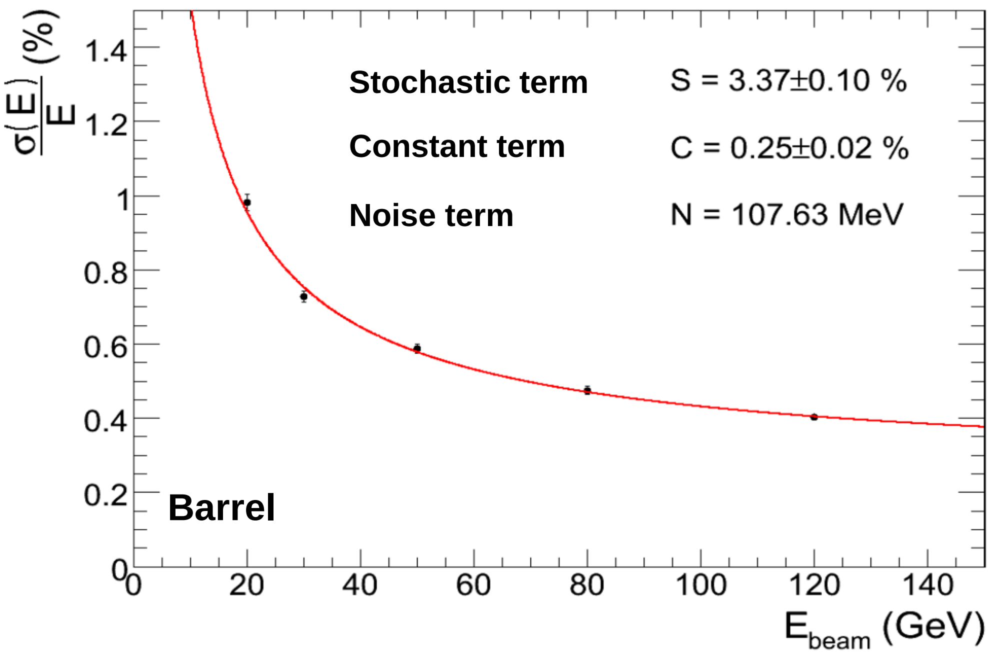

Electron energy resolution as a function of energy

Electrons centrally (4mmx4mm) incident on crystal

Resolution 0.4% at 120 GeV

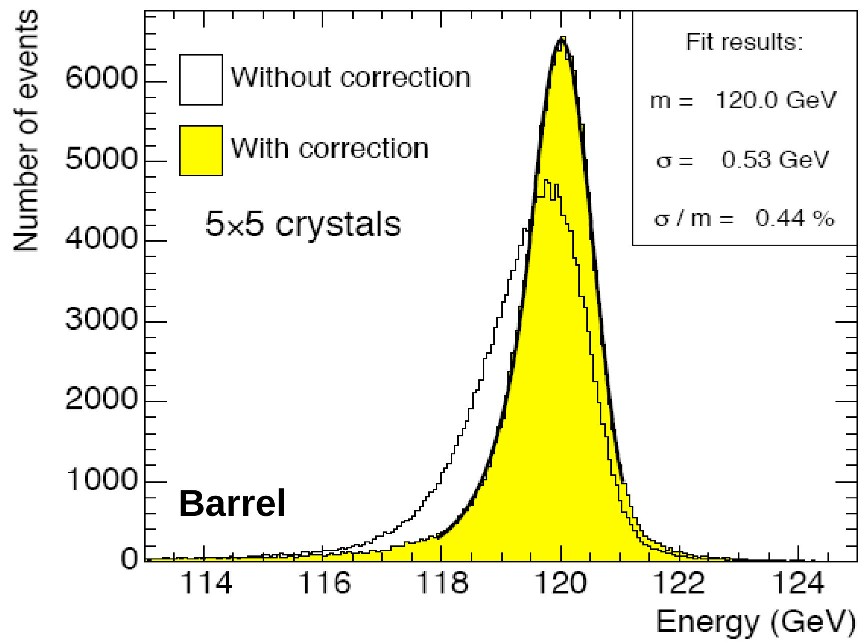

Energy resolution at 120 GeV

Electrons incident over full crystal face

Energy sum over 5x5 array wrt hit crystal.

Universal position 'correction function' for the reconstructed energy applied

Resolution 0.44%

EM showers: transverse profile

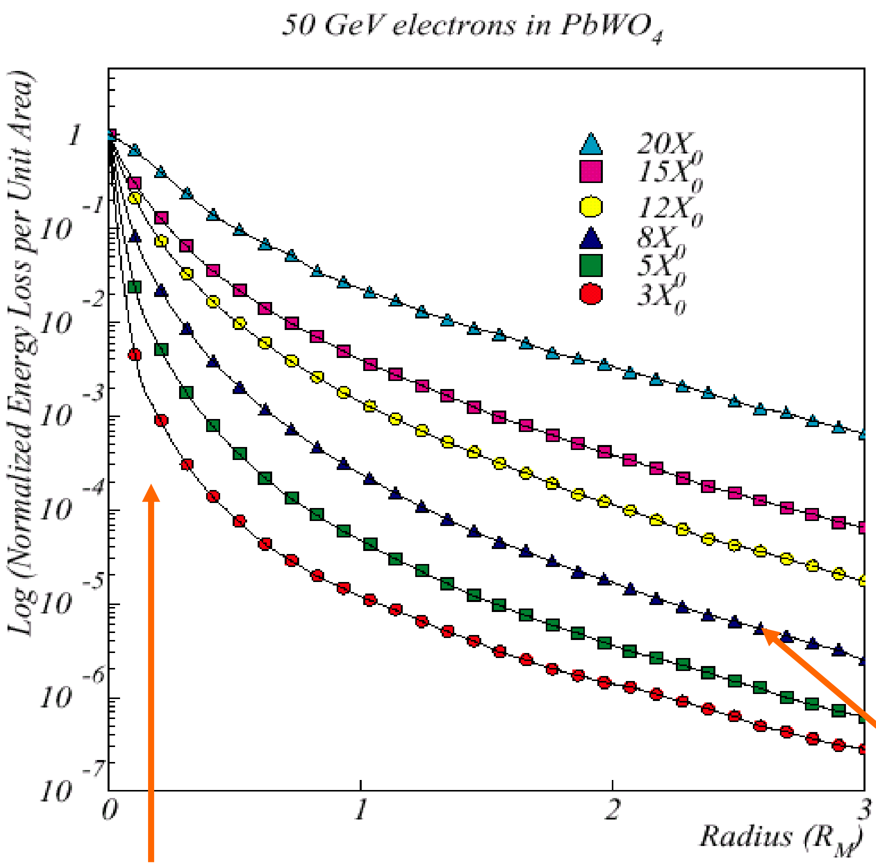

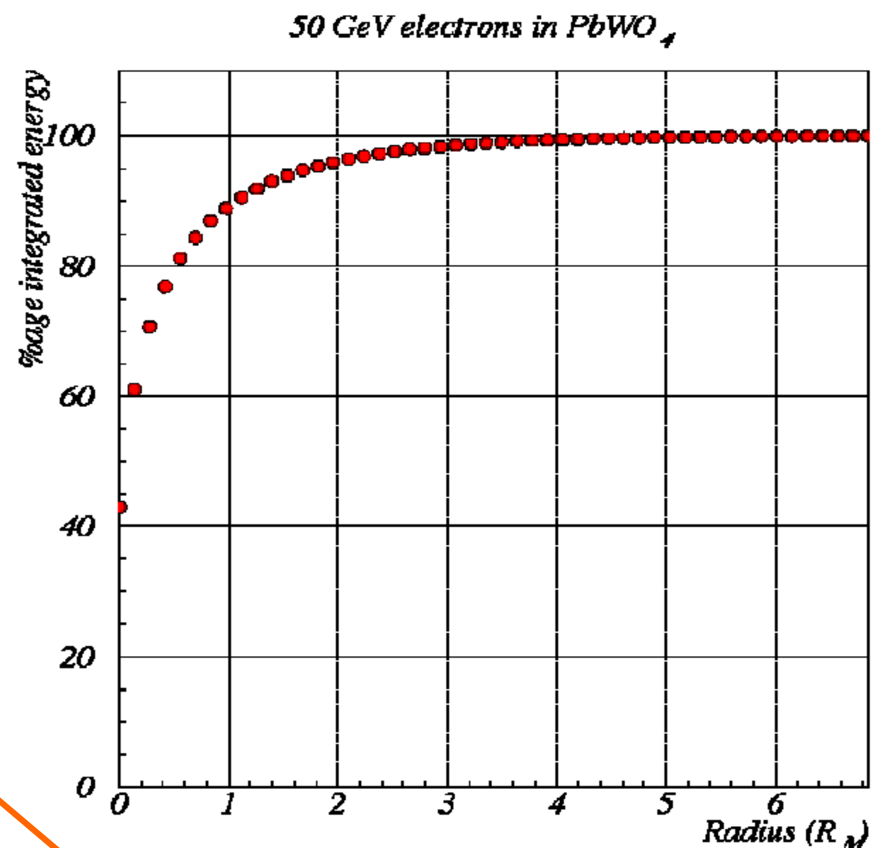

Central core: multiple scattering

Peripheral halo: propagation of less attenuated photons, widens with depth of of the shower

EM showers, logitudinal profile

Material	Z	A	ρ [g/cm³]	X_0 [g/cm²]	λ_a [g/cm²]
Hydrogen (gas)	1	1.01	0.0899 (g/l)	63	50.8
Helium (gas)	2	4.00	0.1786 (g/l)	94	65.1
Beryllium	4	9.01	1.848	65.19	75.2
Carbon	6	12.01	2.265	43	86.3
Nitrogen (gas)	7	14.01	1.25 (g/l)	38	87.8
Oxygen (gas)	8	16.00	1.428 (g/l)	34	91.0
Aluminium	13	26.98	2.7	24	106.4
Silicon	14	28.09	2.33	22	106.0
Iron	26	55.85	7.87	13.9	131.9
Copper	29	63.55	8.96	12.9	134.9
Tungsten	74	183.85	19.3	6.8	185.0

Shower parametrization

$$\frac{dE}{dt} \propto t^{\alpha} e^{\beta t}$$

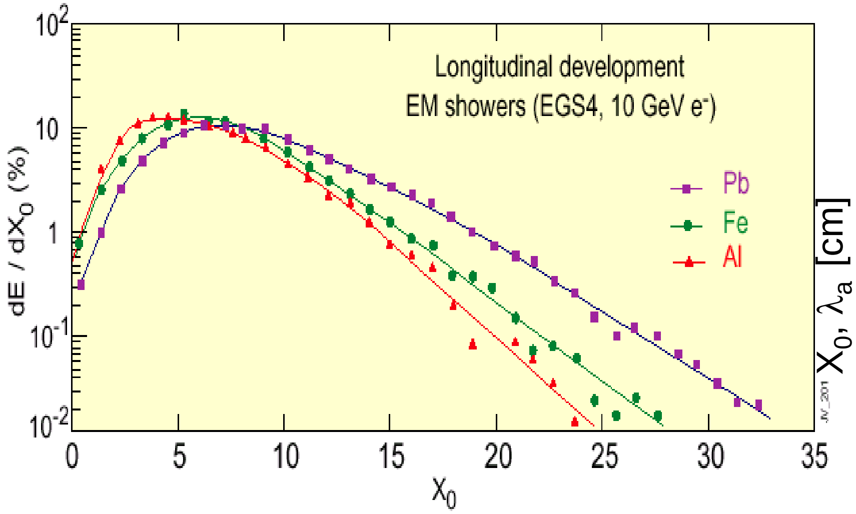

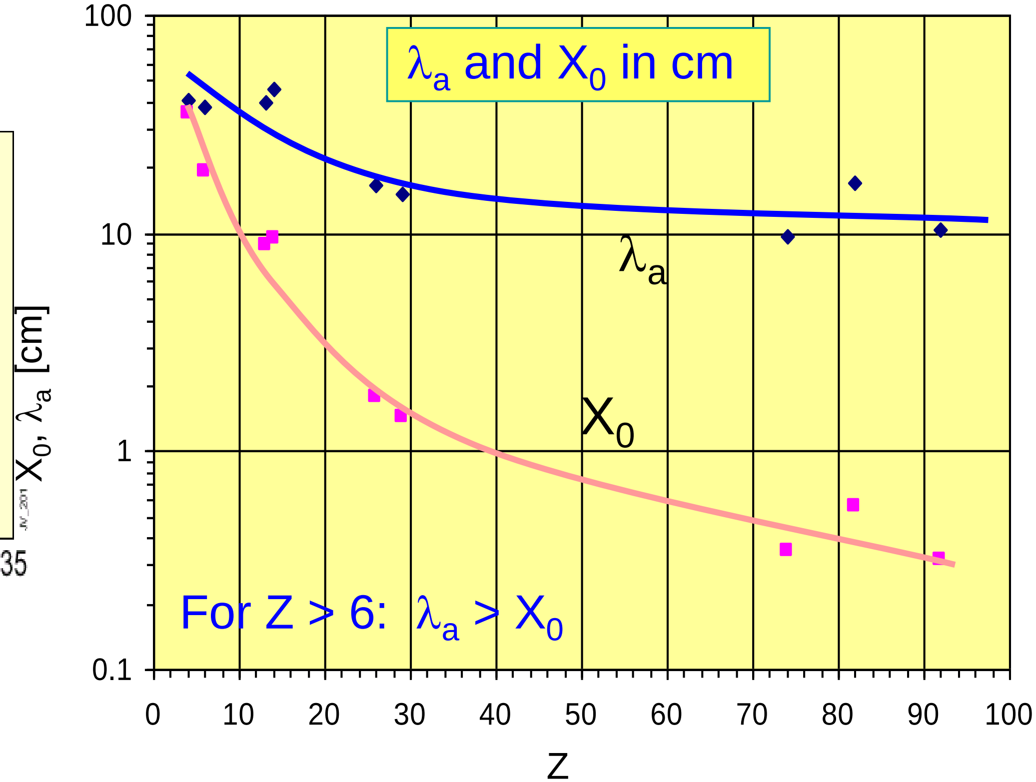

These crystals make light!

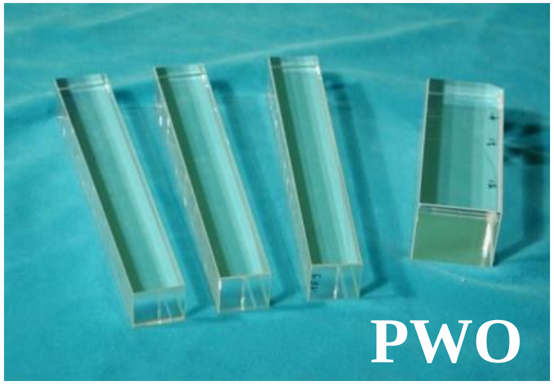

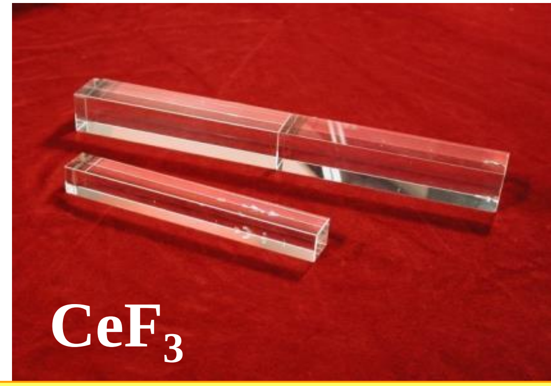

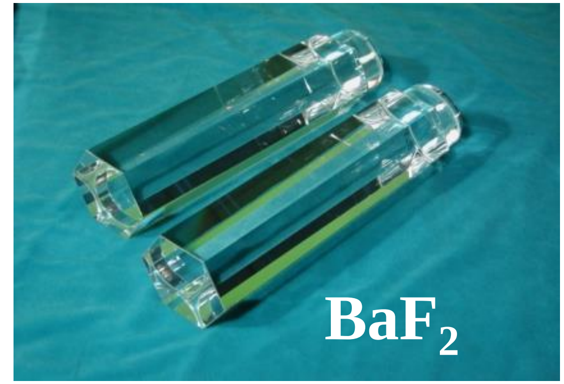

Crystals are basic components of electromagnetic calorimeters aiming at precision

Scintillation: a three step process

Scintillator + Photo Detector = Detector

PMT,PD,APD

How does it works

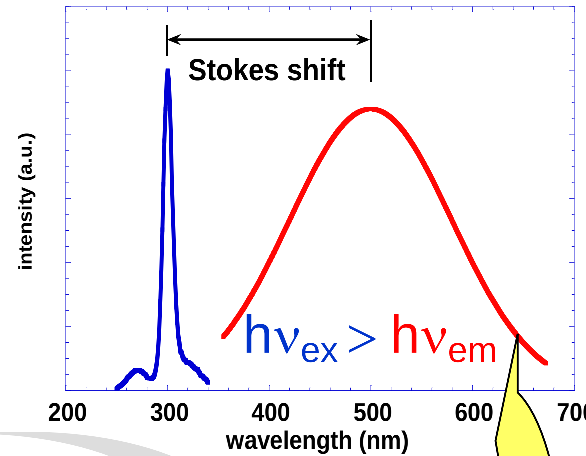

absorption e.g. γ

$$I(E) = I_0(E)e^{-\mu d}$$

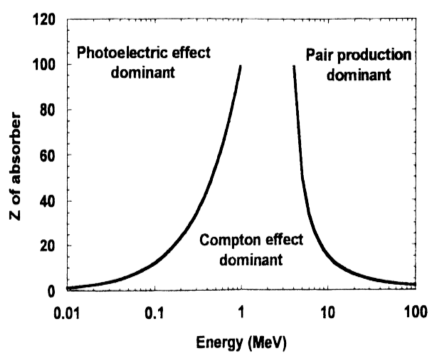

conversion

Energy → Excitation

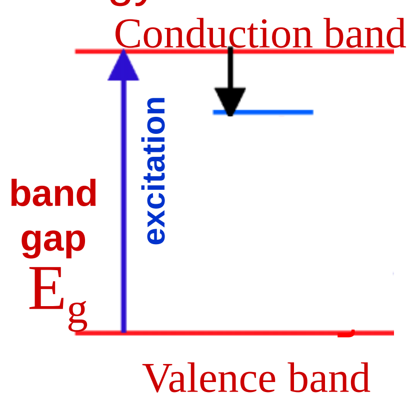

emission

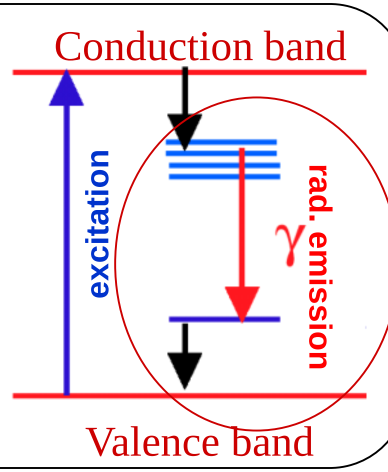

Variation in the lattice
(e.g. defects and impurities)
↓
local electronic energy levels in the energy gap

If these levels are unoccupied electrons moving in the conduction band may enter these centres

The centres are of three main types:

- Luminescence centres in which the transition to the ground state is accompaigned by photon emission
- Quenching centres in which radiationless thermal dissipation of excitation energy may occur
- Traps which have metastable levels from which the electrons may subsequently return to the conduction band by acquiring thermal energy from the lattice vibrations or fall to the valence band by a radiationless transition

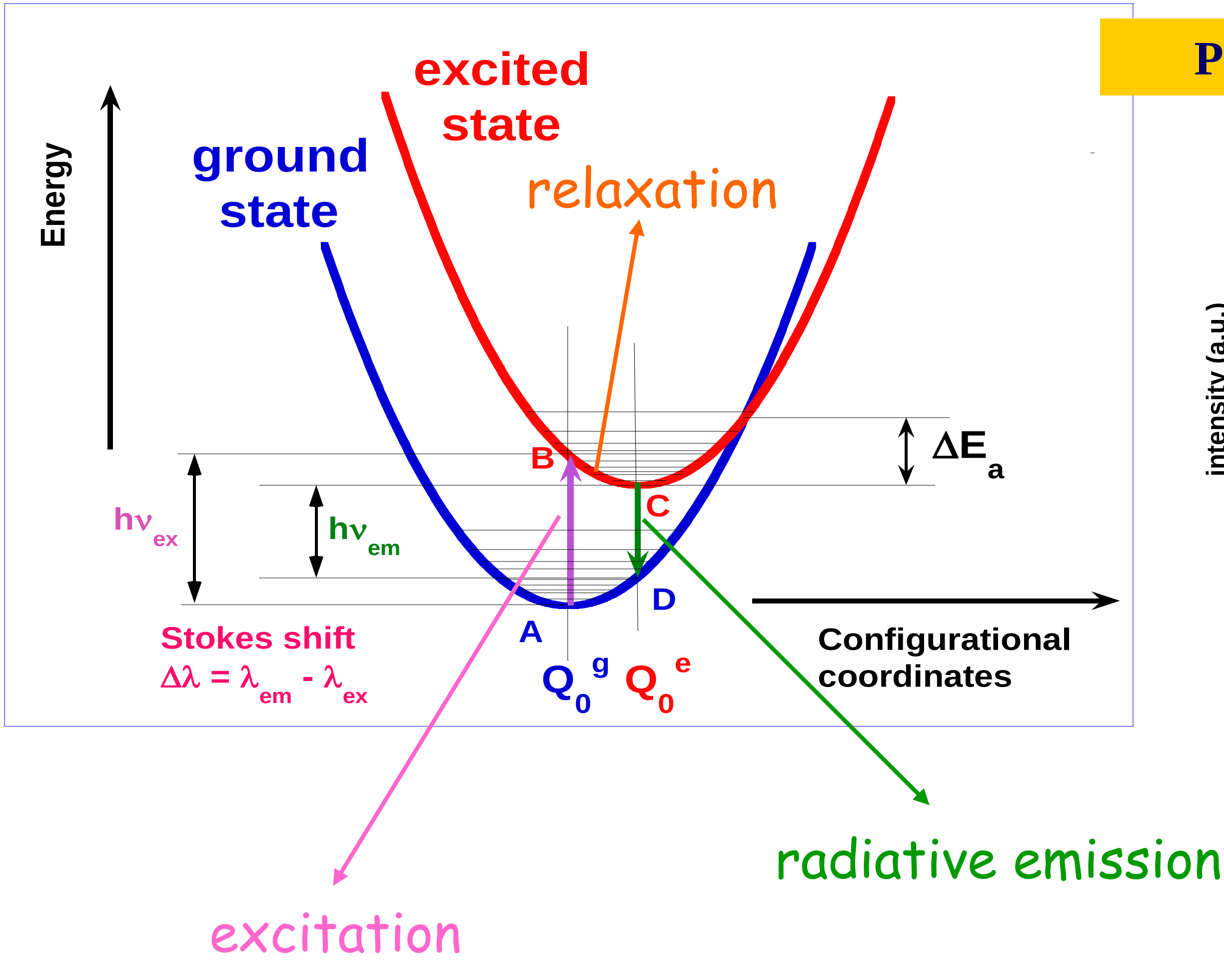

$PbWO_4$: λ_{excit}=300nm ; λ_{emiss}=500nm

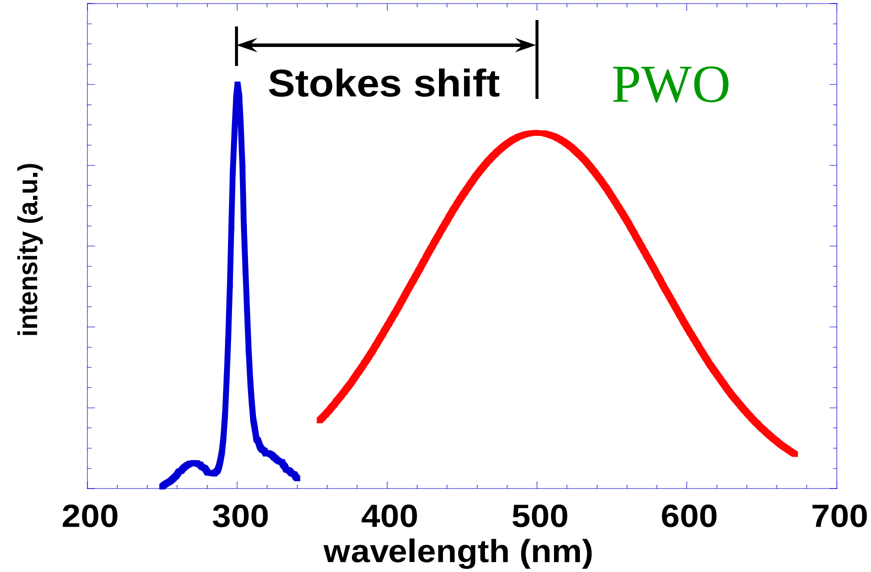

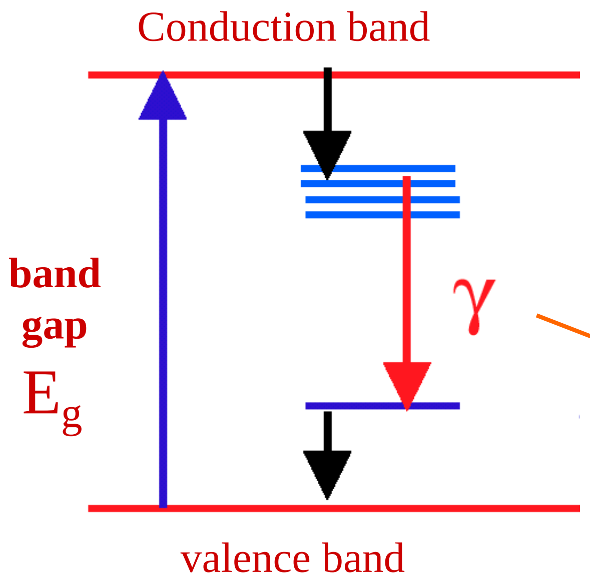

$E_{dep} \rightarrow$ e-h

$E_s = \beta\, E_g \quad \beta > 1$

$N_{eh} = E_{dep} / \beta E_g$

$N_\gamma = SQN_{eh}$

Efficiency of transfer to luminescent centres

radiative efficiency of luminescent centres

$$\eta_\gamma = N_\gamma / E_{dep} = SQN_{eh} / E_{dep} = \mathbf{SQ/\,\beta E_g}$$

- S, Q ≈ 1 , βE_g as small as possible
- medium transparent to λ_{emiss}

CMS Barrel and Endcap Homogeneous ECAL

A CMS Supermodule with 1700 tungstate crystals

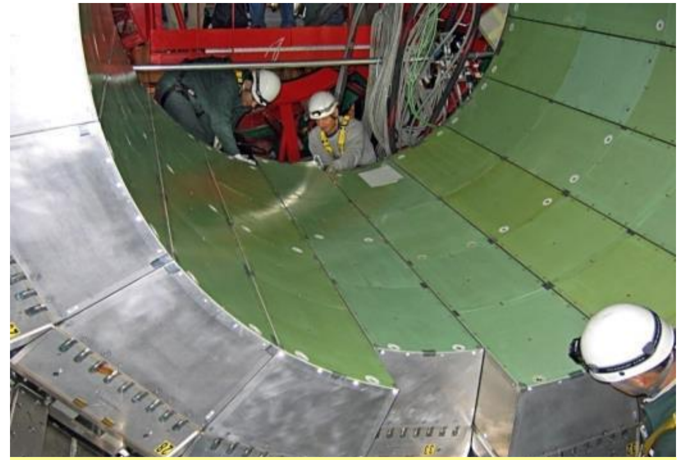

Installation of the last SM into the first half of the barrel

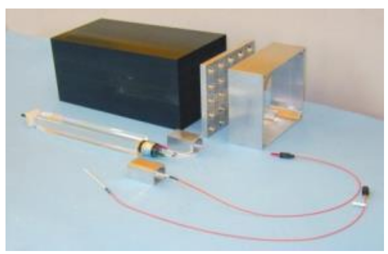

A CMS endcap 'supercrystal' 25 crystals/VPTs

CMS HCAL

Copper has been selected as the absorber material because of its density. The HB is constructed of two half-barrels each of 4.3 meter length. The HE consists of two large structures, situated at each end of the barrel detector and within the region of high magnetic field. Because the barrel HCAL inside the coil is not sufficiently thick to contain all the energy of high energy showers, additional scintillation layers (HOB) are placed just outside the magnet coil. The full depth of the combined HB and HOB detectors is approximately 11 absorption lengths.

The hadron barrel (HB) and hadron endcap (HE) calorimetesr are sampling calorimeters with 50 mm thick copper absorber plates which are interleaved with 4 mm thick scintillator sheets.

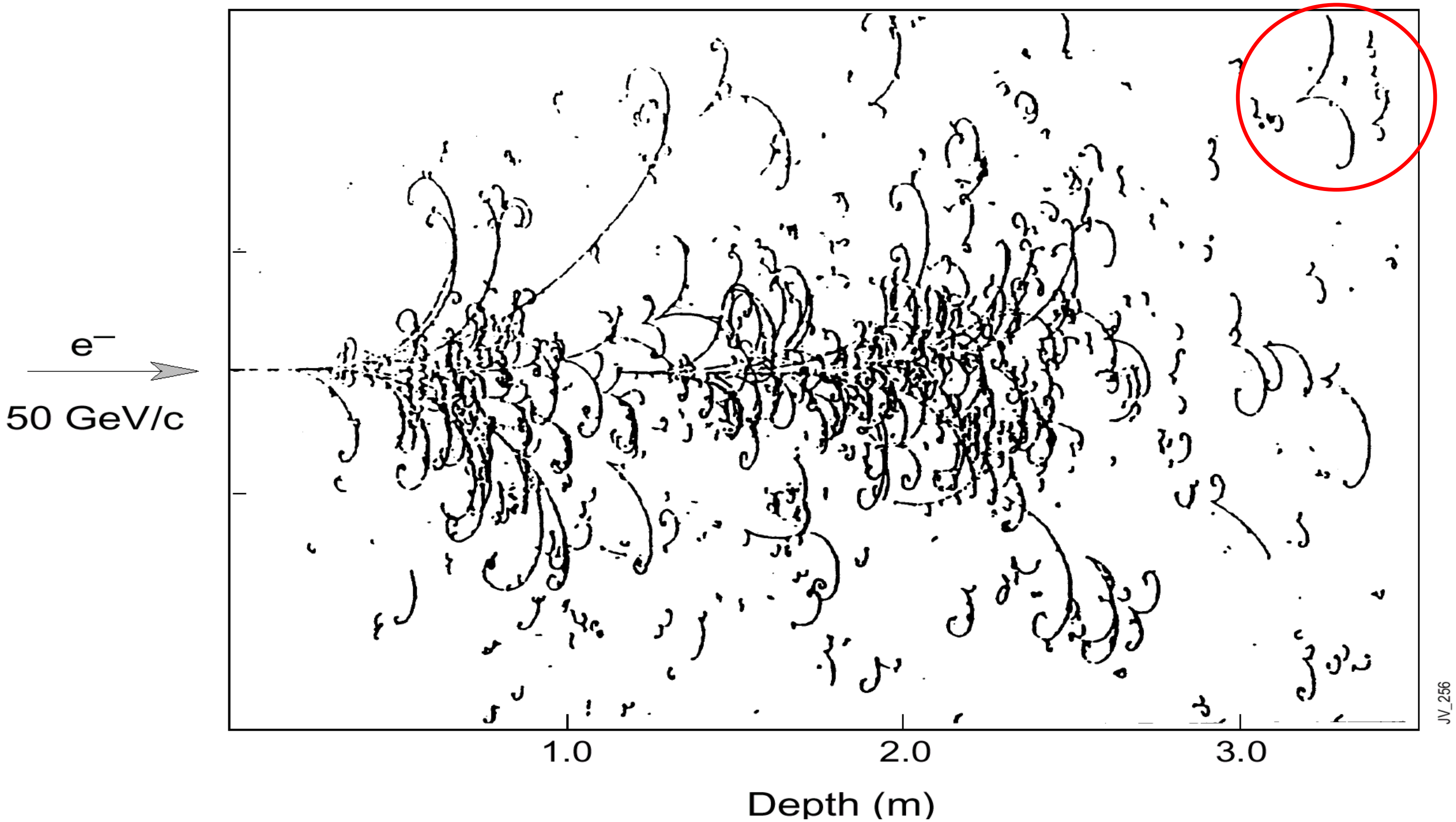

Big European Bubble Chamber filled with Ne:H_2 = 70%:30%, 3T Field, L=3.5 m, X_0≈34 cm, 50 GeV incident electron

✦ We study the inclusive dijet final state using the **dijet mass spectrum** and the **dijet centrality ratio** observables.

✦ Together the Dijet Mass and Ratio provide a **test of QCD** and a **sensitive search** for new physics beyond the Standard Model.

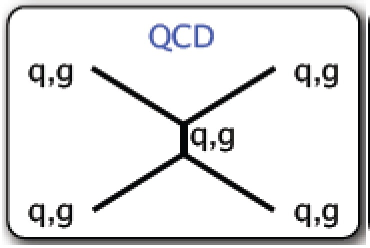

- Dijet mass distribution is a simple check of rate vs dijet mass from QCD and PDFs.
- Dijet centrality ratio is a detailed measure of QCD dynamics from angular distribution.

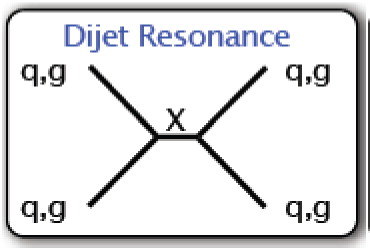

- Dijet mass provides most sensitive *"bump"* hunt for new particles decaying to dijets.
- Dijet centrality ratio can confirm that a *"bump"* is not QCD fluctuation.

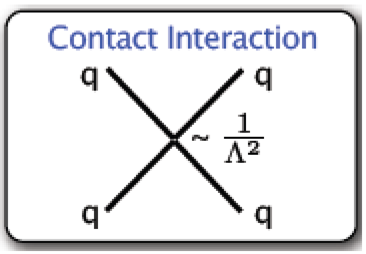

- Dijet centrality ratio is more sensitive than the dijet mass to contact interactions from quark compositeness.
  - when all experimental uncertainties are considered.

Jet Energy Resolution with stand alone calorimetry

For a single hadronic particle: $\sigma_E / E = a / \sqrt{E} \oplus c$ (neglect electronic noise)

Jet with low particle energies, resolution is dominated by a,
and at high particle energies by c

If the stochastic term, a, dominates:
- error on Jet energy ~ same as for a single particle of the same energy

If the constant term dominates:
- error on Jet energy is less than for a single particle of the same energy

For example:
1 TeV jet composed of four hadrons of equal energy
Calorimeter with $\sigma_E / E = 0.3 / \sqrt{E} \oplus 0.05$

$\delta E_{Jet} = 25\ GeV$,
compared to $\delta E = 50\ GeV$, for a single 1 TeV hadron

Jet s in CMS at the LHC, pp collisions at 7TeV

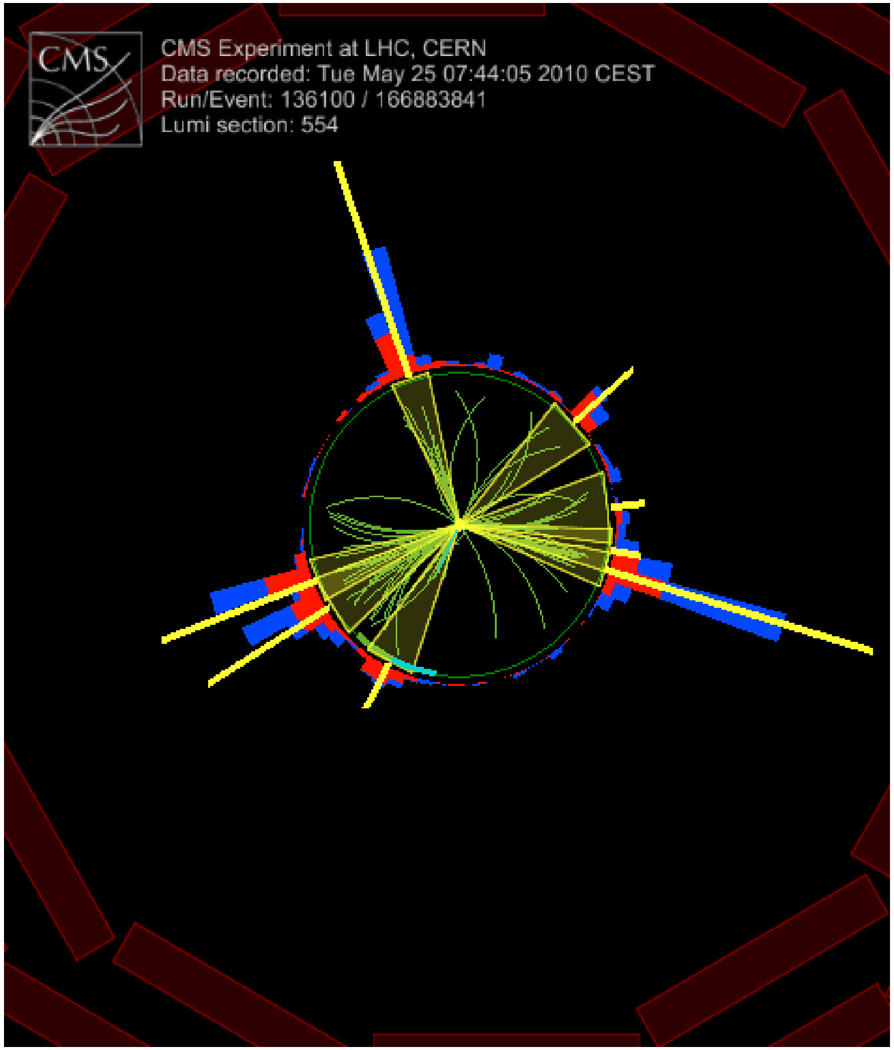

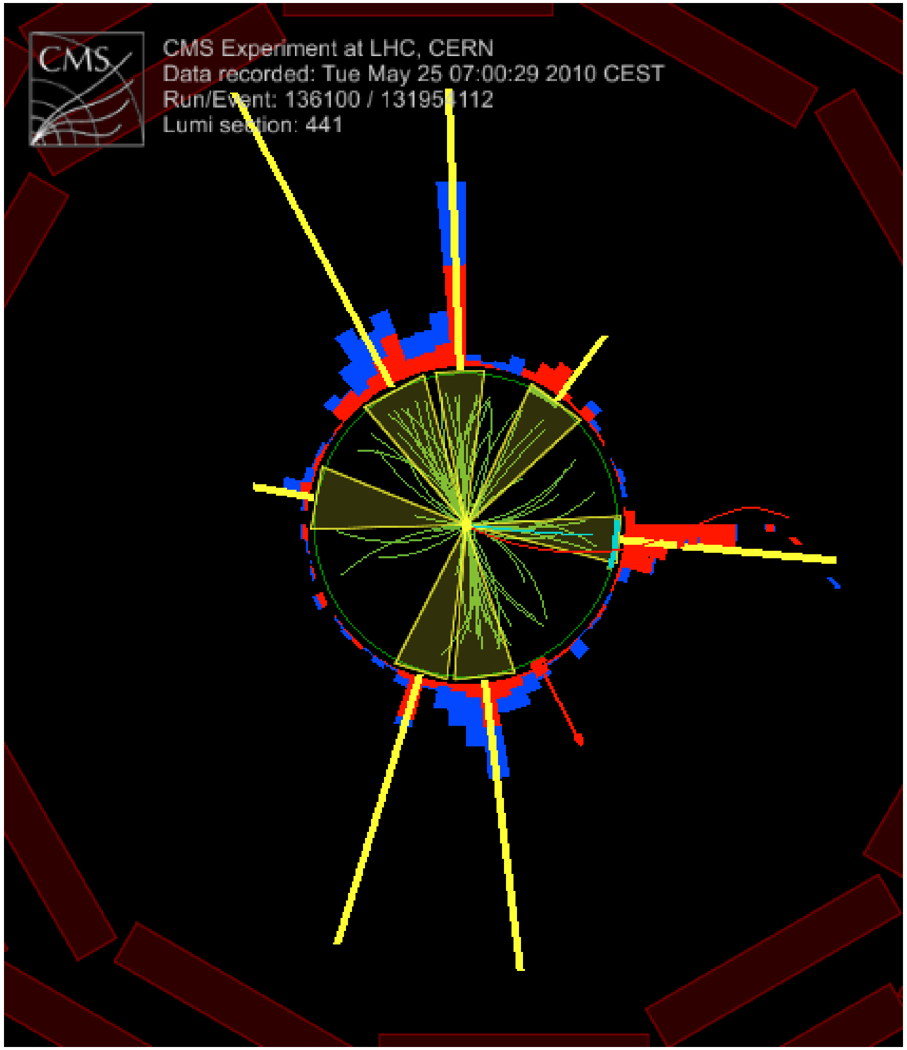

Red - ECAL, Blue - HCAL energy deposits

Yellow – Jet energy vectors